

THE DEFORMATION OF RUBBER CYLINDERS AND TUBES BY ROTATION

P. CHADWICK, C. F. M. CREASY and V. G. HART

(Received 20 September 1976)

(Revised 14 March 1977)

Abstract

A detailed analytical and numerical study is made of the deformation of highly elastic circular cylinders and tubes produced by steady rotation about the axis of symmetry. Explicit results are obtained through the use of Ogden's strain-energy function for incompressible isotropic elastic materials which, as well as being analytically convenient, is capable of reproducing accurately the observed isothermal behaviour of vulcanized rubber over a wide range of deformations. The three problems of steady rotation considered here concern (i) a tube shrink-fitted to a rigid spindle, (ii) an unconstrained tube, and (iii) a solid cylinder. In each case a set of restrictions on the material constants appearing in the strain-energy function is stated which ensures that a tubular or cylindrical shape-preserving deformation exists for all angular speeds and that, for problems (i) and (iii), there is no other solution. In connection with problems (ii) and (iii) values of the material constants are also given which correspond to the bifurcation or non-existence of solutions. Energy considerations are used to determine the local stability of the various solutions obtained.

1. Introduction

In a series of recent papers [4, 5, 11, 12] existence-uniqueness questions have been investigated for a number of deformations, both universal and non-universal, of incompressible isotropic elastic materials having the general form of strain-energy function introduced by Ogden [10]:

$$W = \sum_{n=1}^s \frac{\mu_n}{\alpha_n} (a_1^{\alpha_n} + a_2^{\alpha_n} + a_3^{\alpha_n} - 3). \quad (1.1)$$

Here a_1, a_2, a_3 are the (strictly positive) principal stretches and μ_n and α_n ($n = 1, 2, \dots, s$) are material constants, the μ_n 's having the physical dimensions of stress and the α_n 's being dimensionless. Considerations of stability and physically realistic response lead to the constitutive inequalities

$$\mu_n \alpha_n > 0 \quad \text{for each } n, \quad (1.2)$$

and the shear modulus in infinitesimal deformations from the reference configuration is given by

$$\mu = \frac{1}{2} \sum_{n=1}^s \mu_n \alpha_n. \quad (1.3)$$

We note that (1.1) includes as special cases both the neo-Hookean and Mooney strain-energy functions, the former being obtained when

$$s = 1; \quad \alpha_1 = 2, \quad \mu_1 = \mu, \quad (1.4)$$

and the latter when

$$s = 2; \quad \alpha_1 = 2, \quad \alpha_2 = -2, \quad \mu = \mu_1 - \mu_2. \quad (1.5)$$

In the papers cited above restrictions on the exponents α_n additional to those implied in (1.2) arise as sufficient conditions for the equations determining certain unknown deformation constants to have unique solutions. The present paper continues this general line of enquiry by studying shape-preserving deformations of a circular cylindrical tube and a solid circular cylinder resulting from steady rotation about the axis of symmetry. Three such situations are considered, involving (i) a tube shrink-fitted to a rigid circular cylindrical spindle, (ii) an unconstrained tube, and (iii) a solid cylinder. In each instance the outer curved surface of the deformed body is traction-free and on both of the plane end-faces, normal to the axis of rotation, the resultant force is taken to be zero. Case (ii) may be viewed as following from (i) when the tube turns rapidly enough to leave the spindle, and case (iii) can be regarded as a limit of either (i) or (ii) when the internal radius of the tube approaches zero.

In Section 2 we obtain formal solutions for the problems just described which are universal in the sense of being valid for any incompressible isotropic elastic material. The specialization of this basic analysis to a material possessing the strain-energy function (1.1) is then carried out in Section 3.

The simplest of the three problems, that of the steadily rotating solid cylinder, is treated in Section 4. Here it is shown that the deformation of the cylinder and the stress distribution are completely and uniquely determined for all angular speeds if the exponents satisfy the additional conditions

$$\alpha_n \leq -1 \quad \text{or} \quad \alpha_n \geq 2 \quad \text{for each } n, \quad (1.6)$$

$$\alpha_n < -1 \quad \text{or} \quad \alpha_n > 2 \quad \text{for some } n. \quad (1.7)$$

The neo-Hookean strain-energy function specified by equations (1.4) fails to meet the condition (1.7), while the exponents chosen by Ogden [10] to secure an accurate fit of experimental data of Treloar [14] for vulcanized natural rubber violate (1.6). These and other considerations prompt us in Section 5 to examine the possibility of adjusting the three pairs of material constants derived by Ogden so as to achieve conformity with the restrictions (1.6) and (1.7), but without seriously disturbing the agreement between theory and experiment. Two sets of constants

are obtained, each providing a representation of Treloar's experimental results which is quite close, especially at high strains, but *in toto* somewhat inferior to the fit produced by Ogden.

Sections 6 and 7 are devoted to the analysis and numerical discussion of the two problems involving a rotating tube. For the shrink-fitted tube it is proved analytically in Section 6 that (1.6) are sufficient conditions for the deformation and the stress to be uniquely determined at all angular speeds for which contact between tube and spindle is maintained. In contrast to the cases of the solid cylinder and the shrink-fitted tube, where only one deformation constant has to be found to complete the solution, the problem of the freely revolving tube involves two unknown constants. Section 7, containing the analysis of the unconstrained tube, is accordingly the most complicated part of the paper. Conditions are given which suffice at all speeds of rotation for the existence, but not necessarily the uniqueness, of a solution to the equations specifying the two deformation constants. These requirements are more restrictive than (1.6) and (1.7), and the Mooney material fails to meet them. Separate consideration is given to this exceptional case.

In an appendix the total potential energy of the rotating body is used to determine the local stability of the shape-preserving deformations studied in Sections 4, 6 and 7. Some discussion of the physical behaviour which spinning tubes and cylinders might be expected to display appears at the ends of Sections 4 and 7.

2. Formal solutions

(a) Basic analysis

We consider a circular cylindrical tube having internal radius A , external radius B and length L in its undeformed state and corresponding dimensions a , b and l when deformed. The tube is composed of an incompressible isotropic hyperelastic material of density ρ and the deformation is assumed to be given by

$$\mathbf{r} = \{\lambda^{-1}(R^2 - A^2) + a^2\}^{\frac{1}{2}}, \quad \theta = \Theta + \omega t, \quad z = \lambda Z. \quad (2.1)$$

Here (R, Θ, Z) and (r, θ, z) are respectively referential and spatial coordinates relating to a common cylindrical polar system based upon the axis of symmetry of the tube, λ and ω are positive constants and t denotes the time. The isochoric deformation (2.1) represents a rotation about the axis with constant angular speed ω combined with a radial inflation and an accompanying axial stretch of amount λ . At a representative material point the principal axes of stretch in the current configuration of the tube coincide with the directions of r , θ and z increasing and the principal stretches are given by

$$a_r = \lambda^{-\frac{1}{2}} v^{-\frac{1}{2}}, \quad a_\theta = \lambda^{-\frac{1}{2}} v^{\frac{1}{2}}, \quad a_z = \lambda, \quad (2.2)$$

where

$$v = \frac{\lambda r^2}{R^2} = \frac{\lambda r^2}{\lambda(r^2 - a^2) + A^2}. \quad (2.3)$$

Because of the isotropy of the material the coordinate directions in the spatial system (r, θ, z) also define the principal axes of stress. The only non-zero physical components of the stress tensor σ relative to this system are therefore σ_{rr} , $\sigma_{\theta\theta}$ and σ_{zz} . The constitutive equations characterizing the stress response of the material may be written in terms of the principal stretches and stresses as

$$\sigma_{rr} = -p + a_r \frac{\partial W}{\partial a_r}, \quad \sigma_{\theta\theta} = -p + a_\theta \frac{\partial W}{\partial a_\theta}, \quad \sigma_{zz} = -p + a_z \frac{\partial W}{\partial a_z}, \quad (2.4)$$

where the strain-energy function W per unit volume in the undeformed configuration is a symmetric function, assumed known, of the principal stretches, and the pressure p , associated with the incompressibility constraint, is not determined *a priori* by the deformation. In view of the relations (2.2) the strain energy can be expressed as a function of λ and v :

$$\bar{W}(\lambda, v) \equiv W(\lambda^{-1}v^{-1}, \lambda^{-1}v^{\frac{1}{2}}, \lambda). \quad (2.5)$$

On forming the partial derivatives of \bar{W} and using the constitutive equations (2.4) we then find that

$$\sigma_{\theta\theta} - \sigma_{rr} = 2v \frac{\partial \bar{W}}{\partial v} \quad \text{and} \quad 2\sigma_{zz} - \sigma_{rr} - \sigma_{\theta\theta} = 2\lambda \frac{\partial \bar{W}}{\partial \lambda}. \quad (2.6)$$

In the absence of external body forces it is a consequence of the equations of motion that the stress components are functions of r only satisfying

$$\frac{d\sigma_{rr}}{dr} + \frac{1}{r}(\sigma_{rr} - \sigma_{\theta\theta}) = -\rho\omega^2 r. \quad (2.7)$$

The pointwise vanishing of the traction on the outer cylindrical boundary of the tube and the zero value of the resultant force on the end-faces provide the conditions

$$\sigma_{rr}(b) = 0, \quad \int_a^b \sigma_{zz} r dr = 0. \quad (2.8)$$

Equation (2.7) can be integrated subject to the first boundary condition to yield

$$\sigma_{rr} = - \int_r^b (\sigma_{\theta\theta} - \sigma_{rr}) \frac{dr}{r} + \frac{1}{2} \rho \omega^2 (b^2 - r^2). \quad (2.9)$$

In particular, the radial stress at the inner wall of the tube is given by

$$\sigma_{rr}(a) = - \int_a^b (\sigma_{\theta\theta} - \sigma_{rr}) \frac{dr}{r} + \frac{1}{2} \rho \omega^2 (b^2 - a^2). \quad (2.10)$$

The equation of motion (2.7) can also be written as

$$r(\sigma_{rr} + \sigma_{\theta\theta}) = \frac{d}{dr} (r^2 \sigma_{rr} + \frac{1}{2} \rho \omega^2 r^4).$$

On integrating, with the use of (2.8) and (2.10), we obtain

$$\int_a^b (\sigma_{rr} + \sigma_{\theta\theta}) r dr = a^2 \int_a^b (\sigma_{\theta\theta} - \sigma_{rr}) \frac{dr}{r} + \frac{1}{4} \rho \omega^2 (b^2 - a^2)^2,$$

whereupon the end-face condition (2.8) can be expressed in the more convenient form

$$\int_a^b (2\sigma_{zz} - \sigma_{rr} - \sigma_{\theta\theta}) r dr + a^2 \int_a^b (\sigma_{\theta\theta} - \sigma_{rr}) \frac{dr}{r} + \frac{1}{4} \rho \omega^2 (b^2 - a^2)^2 = 0. \quad (2.11)$$

We conclude this basic analysis by entering into equations (2.9), (2.10) and (2.11) the formulae (2.6) for $\sigma_{\theta\theta} - \sigma_{rr}$ and $2\sigma_{zz} - \sigma_{rr} - \sigma_{\theta\theta}$, at the same time changing the variable of integration from r to v by means of equation (2.3). The results obtained are

$$\sigma_{rr} = - \int_{\chi}^{\{1+(\gamma^{-1}-1)(a/r)^2\}^{-1}} \frac{\partial \bar{W}}{\partial v} \frac{dv}{v-1} + \frac{1}{2} \rho \omega^2 \{ \lambda^{-1} A^2 (N^2 - 1) + a^2 - r^2 \}, \quad (2.12)$$

$$\sigma_{rr}(a) = - \int_{\chi}^{\gamma} \frac{\partial \bar{W}}{\partial v} \frac{dv}{v-1} + \frac{1}{2} \rho \omega^2 \lambda^{-1} A^2 (N^2 - 1), \quad (2.13)$$

and

$$\int_{\chi}^{\gamma} \left\{ \lambda(\gamma-1) \frac{\partial \bar{W}}{\partial \lambda} + \gamma(v-1) \frac{\partial \bar{W}}{\partial v} \right\} \frac{dv}{(v-1)^2} + \frac{1}{4} \rho \omega^2 \lambda^{-1} A^2 (N^2 - 1)^2 = 0, \quad (2.14)$$

where

$$N = B/A (> 1), \quad \gamma = \lambda a^2 / A^2, \quad \chi = (N^2 - 1 + \gamma) / N^2. \quad (2.15)$$

(b) Shrink-fitted tube

When the tube is mounted on a rigid circular cylindrical spindle the internal radius a in the deformed configuration coincides with the radius of the spindle and is thereby known. In this case equation (2.14) in principle determines the axial stretch λ and the deformation is then fully specified. The distribution of stress in the tube is given by equations (2.12) and (2.6), the contact stress at the interface between the tube and the spindle being obtained from equation (2.13). Under shrink-fit conditions the inequality

$$\sigma_{rr}(a) < 0 \quad (2.16)$$

is a necessary condition for the tube to remain in contact with the spindle.

(c) Freely rotating tube

When the tube is allowed to spin freely about its axis the inner as well as the outer curved surface is traction-free and the internal radius a in the deformed configuration is no longer prescribed. In this situation equation (2.14) and (2.13)

(with $\sigma_{rr}(a) = 0$) serve in principle to fix a and λ . The deformation is then completely known and equations (2.12) and (2.6) again specify the non-zero stress components.

(d) *Rotating cylinder*

A formal solution for a circular cylinder, originally of radius B , revolving about its axis with constant angular speed ω can be derived from the results of subsection (a) by letting A and a tend to zero. From equation (2.3) we see that in this limit the variable v is identically equal to unity, whence $\partial\bar{W}/\partial v = 0$ and $\partial\bar{W}/\partial\lambda$ depends on λ only. The integration in equation (2.14) can now be performed explicitly; after dividing through by $(N^2 - 1)\lambda^{-1}$ and then setting $A = 0$ we reach the simple formula

$$\lambda^2 \frac{\partial\bar{W}}{\partial\lambda}(\lambda, 1) + \frac{1}{4}\rho\omega^2 B^2 = 0 \tag{2.17}$$

which determines λ . The distribution of stress is supplied by equations (2.12) and (2.6) in the form

$$\sigma_{rr} = \sigma_{\theta\theta} = \frac{1}{2}\rho\omega^2(\lambda^{-1} B^2 - r^2), \quad \sigma_{zz} = \sigma_{rr} + \lambda \frac{\partial\bar{W}}{\partial\lambda}(\lambda, 1). \tag{2.18}$$

Results equivalent to (2.17) and (2.18) were first obtained by Green and Shield [6, §6].

3. Ogden materials

We now particularize the main results of Section 2 by adopting the Ogden strain-energy function (1.1). The form of the function $\bar{W}(\lambda, v)$ which then follows from the definition (2.5) is

$$\bar{W}(\lambda, v) = \sum_{\alpha_n}^{\mu_n} \{ \lambda^{\alpha_n} + \lambda^{-i\alpha_n} (v^{i\alpha_n} + v^{-i\alpha_n}) - 3 \}, \tag{3.1}$$

where, from this point onwards, summation over the range $1, \dots, s$ of the subscript n is not indicated explicitly. Recorded below, without detailed derivations, are the formulae to be used later.

(a) *Shrink-fitted tube*

We introduce the inflation constant

$$q = a/A (> 1), \tag{3.2}$$

and regard $\gamma = \lambda q^2$ rather than λ as the quantity determined by equation (2.14). The result of substituting (3.1) into this equation and replacing λ by $q^{-2}\gamma$ can be arranged as

$$J(\gamma) \equiv \mu_n j(\gamma; \alpha_n) = -\frac{1}{2}\rho\omega^2 A^2 (N^2 - 1)^2, \tag{3.3}$$

where

$$j(\gamma; \alpha) = q^{-2+\alpha} \gamma^{1-\frac{1}{2}\alpha} \{ \gamma I_1(\gamma; \alpha) - (\gamma - 1) I_2(\gamma; \alpha) \} + 2(N^2 - 1)(q^{-2-2\alpha} \gamma^{1+\alpha} - q^{-2+\alpha} \gamma^{1-\frac{1}{2}\alpha}) \tag{3.4}$$

and

$$I_1(\gamma; \alpha) = \int_x^\gamma \frac{v^{\frac{1}{2}\alpha} - v^{-\frac{1}{2}\alpha}}{v(v-1)} dv, \quad I_2(\gamma; \alpha) = \int_x^\gamma \left(\frac{v^{\frac{1}{2}\alpha} - v^{-\frac{1}{2}\alpha}}{v-1} \right)^2 dv. \tag{3.5}$$

The contact stress, as given by equations (2.13) and (3.1), is

$$\sigma_{rr}(a) = -\frac{1}{2} \mu_n q^{\alpha_n} \gamma^{-\frac{1}{2}\alpha_n} I_1(\gamma; \alpha_n) + \frac{1}{2} \rho \omega^2 q^2 A^2 (N^2 - 1) \gamma^{-1}. \tag{3.6}$$

(b) *Freely rotating tube*

In this case two equations for λ and γ are obtained from equations (2.13) and (2.14) by putting $\sigma_{rr}(a) = 0$ and inserting the expression (3.1). After a little manipulation, aimed at eliminating the integral I_1 from the equation derived from (2.14), this pair of equations can be set out as

$$K(\lambda, \gamma) \equiv \mu_n \lambda^{1-\frac{1}{2}\alpha_n} I_1(\gamma; \alpha_n) = \rho \omega^2 A^2 (N^2 - 1), \tag{3.7}$$

$$L(\lambda, \gamma) \equiv \frac{\mu_n}{N^2 - 1 + 2\gamma} \{ 2(N^2 - 1)(\lambda^{1+\alpha_n} - \lambda^{1-\frac{1}{2}\alpha_n}) - \lambda^{1-\frac{1}{2}\alpha_n} (\gamma - 1) I_2(\gamma; \alpha_n) \} = -\frac{1}{2} \rho \omega^2 A^2 (N^2 - 1). \tag{3.8}$$

When λ and γ are known the internal radius a of the deformed tube is given by equation (3.2), the inflation constant q being $(\gamma/\lambda)^{\frac{1}{2}}$.

(c) *Rotating cylinder*

Equation (2.17), in conjunction with (3.1), gives the following relation for the axial stretch λ :

$$M(\lambda) \equiv \mu_n (\lambda^{1+\alpha_n} - \lambda^{1-\frac{1}{2}\alpha_n}) = -\frac{1}{2} \rho \omega^2 B^2. \tag{3.9}$$

4. The rotating cylinder

(a) *Existence and uniqueness of solutions*

We turn now to a discussion of the solutions of equation (3.9). On account of the constitutive inequalities (1.2) it follows from the definition of the function M that $M(\lambda) \geq 0$ according as $\lambda \geq 1$. Thus, for $\omega > 0$, any solution of (3.9) lies in the interval $0 < \lambda < 1$, which means that rotation necessarily causes axial shortening of the cylinder.

A necessary and sufficient condition for equation (3.9) to have a solution for all $\omega \geq 0$ is that $M(\lambda)$ takes on all negative values as λ varies between 0 and 1. This is so if and only if $M(\lambda) \rightarrow -\infty$ as $\lambda \downarrow 0$ which is in turn true if and only if the exponents α_n have the property (1.7). Granted the inequalities (1.2), (1.7) is therefore a necessary and sufficient condition for equation (3.9) to determine at least one value of λ for all $\omega \geq 0$.

The number of solutions of (3.9) is at most one for all speeds of rotation if and only if M is a monotone function for $0 < \lambda < 1$. Since

$$M'(\lambda) = \mu_n\{(\alpha_n + 1)\lambda^{\alpha_n} + (\frac{1}{2}\alpha_n - 1)\lambda^{-\frac{1}{2}\alpha_n}\}, \tag{4.1}$$

the requirements (1.6) are sufficient for M to be monotone; as will appear in subsection (c), however, they are not necessary conditions. In any range of values of ω for which a solution of (3.9) exists the monotonicity of M ensures not only the uniqueness of the solution but also that λ decreases as ω increases.

When the conditions (1.6) and (1.7) are both fulfilled we now see that equation (3.9) yields a unique value of the unknown deformation constant λ no matter what the speed of rotation of the cylinder. This justifies the statement made in Section 1.

(b) *Particular materials*

The neo-Hookean solid specified by equations (1.4) meets the requirement $\alpha_1 \geq 2$ imposed by (1.6) but fails to satisfy (1.7). From the preceding discussion we deduce that a positive solution of equation (3.9) can exist for at most a limited range of angular speeds and that when it exists the solution is unique. In fact (3.9) can be solved explicitly in this case to give

$$\lambda = \left(1 - \frac{\omega^2}{\omega_0^2}\right)^{\frac{1}{2}} \tag{4.2}$$

where $\rho\omega_0^2 B^2 = 4\mu$. As the speed of rotation increases the axial stretch decreases from unity when $\omega = 0$ to zero when $\omega = \omega_0$, at which juncture the cylinder has collapsed into a lamina of zero thickness and infinite radius. This plainly constitutes physically unrealistic behaviour and we recall that a similar instance of a neo-Hookean elastic material losing its resistance to deformation occurs in the spherically symmetric motion resulting from the sudden application of pressure at an internal boundary [9, §7; 3, §3].

When the cylinder is made of a Mooney material equations (1.5) apply, with

$$\mu_1 > 0, \quad \mu_2 < 0 \tag{4.3}$$

(on account of the inequalities (1.2)) and the conditions (1.6) and (1.7) are both satisfied. Equation (3.9) accordingly yields a unique value of λ for all $\omega \geq 0$. This conclusion, first reached by Green and Zerna [7, p. 103], is illustrated in Fig. 1 where curve (b) depicts the variation of $-\mu^{-1}M(\lambda)$ with λ for a Mooney material with constants $\mu_1 = \frac{1}{2}\mu$, $\mu_2 = -\frac{1}{2}\mu$. With the use of the definition ω_0 equation (3.9) becomes

$$-\mu^{-1}M(\lambda) = (\omega/\omega_0)^2, \tag{4.4}$$

and inspection of curve (b) at once confirms the existence of precisely one solution for all speeds of rotation. In contrast, curve (a), referring to a neo-Hookean material, shows that no physically meaningful solution of (4.4) exists when $\omega \geq \omega_0$.

In the three-term strain-energy function of the form (1.1) used by Ogden [10, §4] to account for the observed stress response of vulcanized natural rubber the material constants are

$$\left. \begin{aligned} \mu_1 &= 6.3, & \mu_2 &= -0.1, & \mu_3 &= 0.012, \\ \alpha_1 &= 1.3, & \alpha_2 &= -2.0, & \alpha_3 &= 5.0, \end{aligned} \right\} \quad (4.5)$$

the μ_n 's being in kg cm^{-2} . The exponents in (4.5) comply with (1.7), but α_1 violates (1.6). A solution of equation (3.9) (or (4.4)) therefore exists for all $\omega \geq 0$, but its

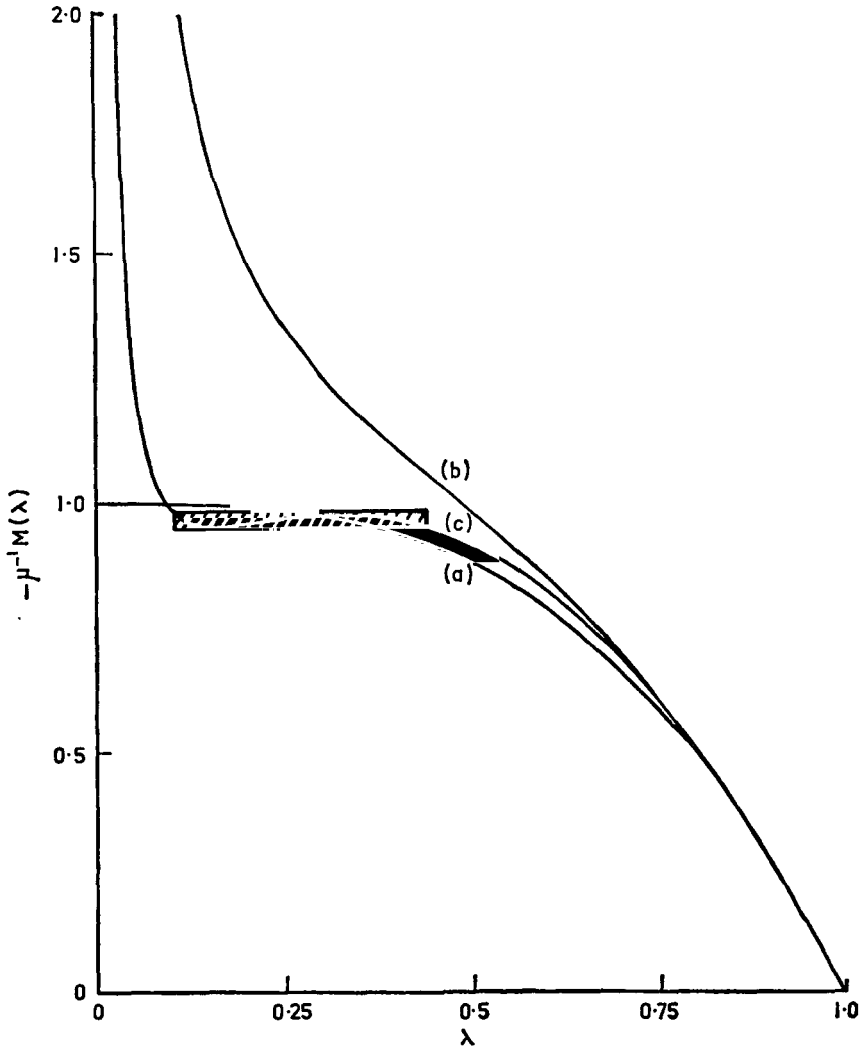


Fig. 1. Rotating cylinder: behaviour of the function $-\mu^{-1}M(\lambda)$ for (a) a neo-Hookean material, (b) a Mooney material with $-\mu_2/\mu_1 = \frac{1}{2}$, and (c) the Ogden material with constants specified in equations (4.5).

uniqueness is not assured. From the variation of $-\mu^{-1}M(\lambda)$ with λ , displayed as curve (c) in Fig. 1, we see that there is a closed interval of values of ω/ω_0 within which equation (4.4) has either two or three solutions. The region of non-uniqueness, shown shaded in Fig. 1, is given by

$$0.104 \leq \lambda \leq 0.434, \quad 0.977 \leq \omega/\omega_0 \leq 0.990. \quad (4.6)$$

(A similar multiplicity of solutions occurs in the inflation of a spherical balloon [1].) As ω increases from zero the cylinder extends radially and shortens axially, the increment of deformation corresponding to a given increase in ω rising steadily. This tendency, reflecting a progressive “softening” of the material, becomes especially pronounced as ω approaches the critical value† ω_0 .

Previous studies of isothermal deformations of Ogden materials yield results for the solid specified by equations (4.5) which agree qualitatively with their counterparts for a Mooney material [4, 5, 11, 12]. Here, however, we have encountered a situation in which the two materials respond differently to prescribed inertial forces.

(c) Discussion

From the energy considerations described in Appendix 2 it may be concluded that in the case of the Mooney material the solution of equation (3.9) is locally stable and that the same is true for the neo-Hookean material when $\omega < \omega_0$. For the Ogden material defined by equations (4.5) there is one stable solution when ω lies outside the interval (4.6). When ω falls within this interval the extreme values of λ are associated with stable solutions and the intermediate value of λ gives an unstable solution. The end-points of the interval (4.6) correspond to one stable and one neutrally stable solution.

It should be emphasized that all the results obtained in this section rest on the assumption that the deformation depends only on the radial coordinate r . Recent work of Patterson and Hill [13] for a rotating neo-Hookean cylinder shows that an alternative axisymmetric mode of deformation dependent on r and z is possible at a value of ω considerably less than ω_0 , and it is conjectured that the physically unrealistic response exhibited by the neo-Hookean cylinder at $\omega = \omega_0$ may be avoided by preference for this alternative mode. In considering the physical behaviour of a rotating cylinder composed of a rubber-like material the possibility of asymmetric deformations must evidently be entertained. (A static case has been studied by Alexander [2].) Thus while the present results are valid when the cylinder deforms in a shape-preserving manner, there is no guarantee that this

† When $\rho = 906.5 \text{ kg m}^{-3}$, $\mu = 4.143 \times 10^5 \text{ Nm}^{-2}$ and $B = 30 \text{ mm}$, we have $\omega_0 = 1425 \text{ s}^{-1} = 13\,610 \text{ r.p.m.}$ For the solid cylinder the principal stretches a_r and a_θ are both equal to λ^{-1} . When $\lambda = 0.104$, $a_r = a_\theta = 3.101$.

represents a close approximation to the conditions realized in practice over the entire range of angular speeds considered in our numerical results. Experimental evidence bearing on this question appears to be lacking.

By adjustment of the material constants in (4.5) it may be possible to remove the non-uniqueness displayed in Fig. 1(c). There then comes into question the extent to which the close correlation of theory and experiment achieved by Ogden [10] is preserved. To take a particular example, the function $M(\lambda)$ is made monotone by reducing μ_1 to 5.49 kg cm^{-2} and increasing α_1 to 1.49 without changing the other four constants.† The 53 readings comprising Treloar's experimental data for vulcanized natural rubber are still represented with fairly good accuracy, but the modification which has been carried out must be regarded as *ad hoc* in as much as no general uniqueness criterion, such as (1.6), has been satisfied. In the next section we look into the possibility of recalculating the material constants in a more systematic way.

5. Re-correlation of theory and experiment for vulcanized natural rubber

In the light of the additional conditions (1.6) the offending exponent in the material constants (4.5) derived by Ogden [10, §4] is $\alpha_1 = 1.3$. An objection to this value can also be raised on more general grounds. Through the attribution of Gaussian statistics to the molecular chains the kinetic theory of rubber elasticity gives strong support to the neo-Hookean form (1.4) of the strain energy as the correct representation of the stress response of a cross-linked rubbery polymer at small strains [15, Ch. 4]. But the neo-Hookean function fails to account satisfactorily for the observed force-extension behaviour of such materials outside the small-strain régime, and the notion of a "non-Gaussian" contribution to the strain energy, supplementing the neo-Hookean function and assuming increasing importance at progressively larger strains, is consequently favoured. When the material constants have the values (4.5) the strain-energy function (1.1) contains no neo-Hookean term. However, the structure "neo-Hookean term + non-Gaussian contribution" can be induced by requiring the first exponent α_1 to be equal to 2, a step involving no conflict with the requirements (1.6). Guided by these considerations and the arguments developed in Section 4(c) we now attempt to correlate Treloar's experimental results [14] with theoretical calculations based upon a three-term strain-energy function of the form (1.1) in which $\alpha_1 = 2$ and the conditions (1.2), (1.6) and (1.7) are all satisfied.

Treloar's data were obtained in three distinct experiments on samples cut from a single sheet of a natural rubber vulcanizate. In each experiment a homogeneous deformation was realized and the load f needed to effect the strain (and reckoned

† This example substantiates our earlier statement that (1.6) are not necessary conditions for equation (4.4) to have a unique solution.

per unit undeformed area) was measured at a sequence of values of the appropriate principal stretch a . The three deformations, simple tension, pure shear and equibiaxial tension, are referred to here as experiments 1, 2 and 3 respectively. The theoretical relations between f and a for the three experimental situations derived from the strain-energy function (1.1) are

$$f = \mu_n p(a; \alpha_n), \quad (5.1)$$

where

$$p(a; \alpha_n) = \begin{cases} a^{-1+\alpha_n} - a^{-1-\frac{1}{2}\alpha_n} & \text{for experiment 1,} \\ a^{-1+\alpha_n} - a^{-1-\alpha_n} & \text{for experiment 2,} \\ a^{-1+\alpha_n} - a^{-1-2\alpha_n} & \text{for experiment 3,} \end{cases} \quad (5.2)$$

see [10, §3]. The values of f calculated from (5.1) and (5.2) using the measured stretches and the material constants specified in (4.5) provide the graphs in Fig. 2 (solid lines), the experimental points being shown by circles, squares and diamonds for experiments 1, 2 and 3 respectively. (This convention is also used in Figs. 3 and 4.) In these figures f_e denotes the experimental and f_t a theoretical value of f , the units being in kg force per cm², and error estimates for the theoretical fit of each set of experimental points are noted in the figure captions.

Following the pattern of equations (4.5) we take α_2 to be less than -1 and α_3 to be large and positive. The exponents then comply with the requirements (1.6) and (1.7), and the constitutive inequalities (1.2) hold provided that μ_1 and μ_3 are positive and μ_2 negative.

At small strains ($a \approx 1$) the main contribution to the load f comes from the first term $\mu_1 p(a; 2)$ with $\mu_2 p(a; \alpha_2)$ next in importance and $\mu_3 p(a; \alpha_3)$ of least importance. We therefore make a preliminary calculation of μ_1, μ_2 and α_2 as follows. First we specify α_2 and evaluate μ_1 and μ_2 by minimizing

$$S = \sum \{f_e - \mu_1 p(a; 2) - \mu_2 p(a; \alpha_2)\}^2,$$

where the sum is over all the data for which $1 < a < 3.5$. Then we find the value of α_2 which gives the smallest minimum value of S . The result of this procedure is the set of values

$$\mu_1 = 3.0 \text{ kg cm}^{-2}, \quad \mu_2 = -0.81 \text{ kg cm}^{-2}; \quad \alpha_1 = 2, \quad \alpha_2 = 1.2. \quad (5.3)$$

At large strains ($a > 5$, say) the expression (5.1) for f is dominated by the third term $\mu_3 p(a; \alpha_3)$ which, for all three experiments, is nearly equal to $\mu_3 a^{-1+\alpha_3}$. The constants μ_3 and α_3 can be estimated for each experiment by fitting a straight line to the plot of $\log\{f_e - \mu_1 p(a; 2) - \mu_2 p(a; -1.2)\}$ versus $\log a$, utilizing all the data for which $a > 3.5$. The plots furnished by experiments 1 and 2 are found to lie reasonably close to the same straight line but the points supplied by experiment 3 fall near to a different line. We therefore compromise by restricting the range of stretches to $a > 4.3$ and excluding data from experiment 3. The values $\mu_3 = 3.7 \times 10^{-5} \text{ kg cm}^{-2}$, $\alpha_3 = 7.8$ are then obtained. At this stage the large-strain results for experiments 1 and 2 turn out to be accurately reproduced, but the last three values of f for

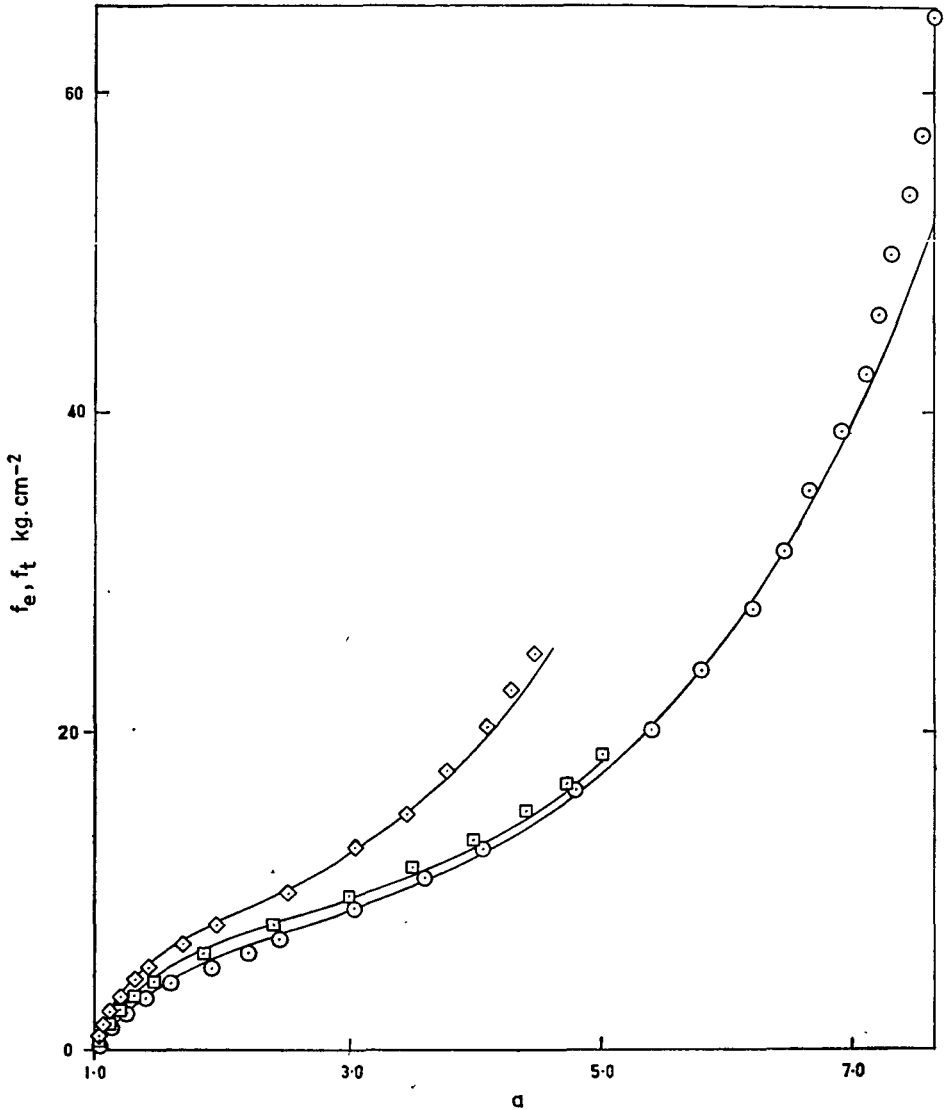


Fig. 2. Comparison with experiment of the response of the Ogden material specified by equations (4.5). The values of $\sum |f_e - f_t|$ for experiments 1, 2, 3 are 41.99 (24 points), 3.95 (13 points), 5.79 (16 points).

experiment 3 are under-estimated. Marginal adjustments produce a slightly better overall fit and the material constants finally chosen are

$$\left. \begin{aligned} \mu_1 = 3.0, \quad \mu_2 = -0.81, \quad \mu_3 = 3.7 \times 10^{-5} \text{ (kg cm}^{-2}\text{)}, \\ \alpha_1 = 2, \quad \alpha_2 = -1.25, \quad \alpha_3 = 7.82. \end{aligned} \right\} \quad (5.4)$$

These constants, entered into equations (5.1) and (5.2), provide the comparison with experiment shown in Fig. 3.

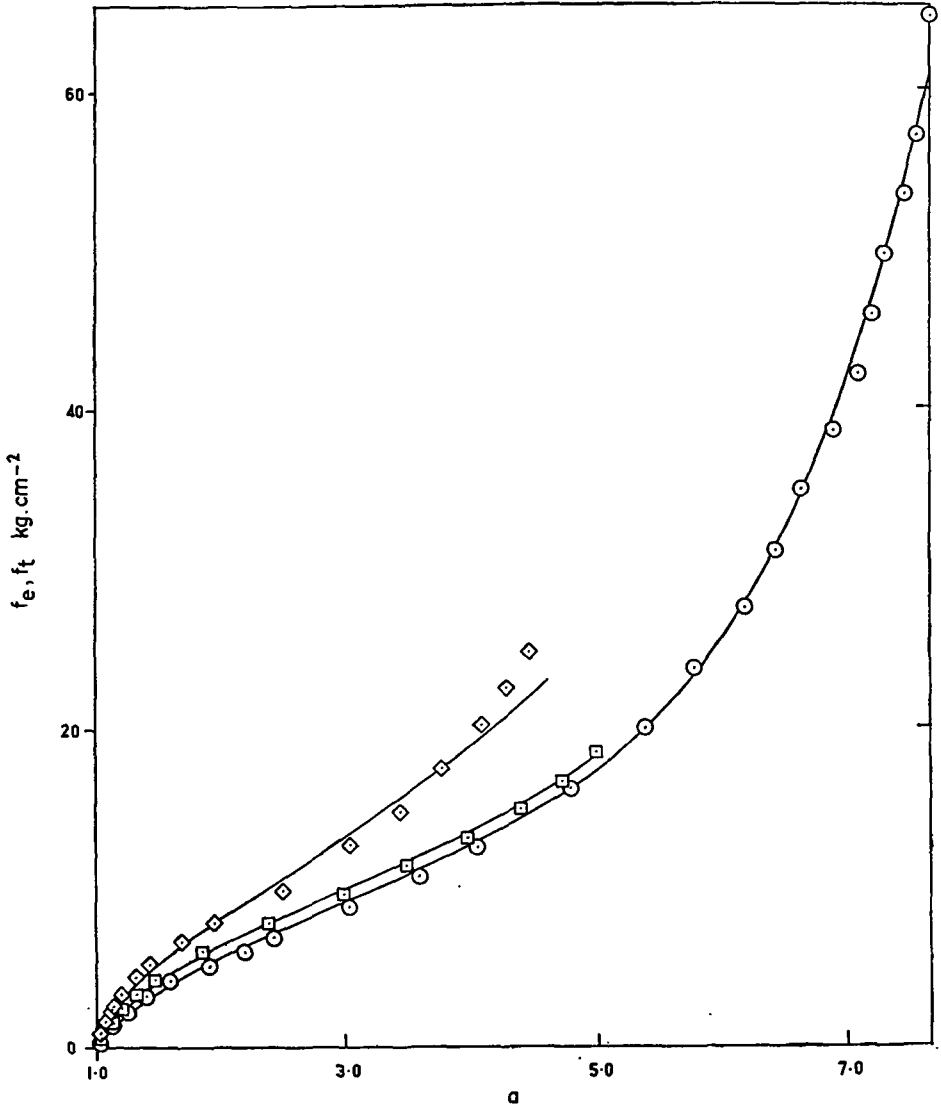


Fig. 3. Comparison with experiment of the response of the modified neo-Hookean material specified by equations (5.4). The values of $\sum |f_e - f_t|$ for experiments 1, 2, 3 are 12.75 (24 points), 2.94 (13 points), 11.05 (16 points).

On repeating the above calculations with $\alpha_1 = 2$ and $\alpha_2 = -2$ *ab initio* we arrive at a second set of material constants, *viz.*

$$\left. \begin{aligned} \mu_1 &= 3.24, & \mu_2 &= -0.1, & \mu_3 &= 6.2 \times 10^{-6} \text{ (kg cm}^{-2}\text{)}, \\ \alpha_1 &= 2, & \alpha_2 &= -2, & \alpha_3 &= 8.7. \end{aligned} \right\} \quad (5.5)$$

The resulting comparison with experiment is presented in Fig. 4.

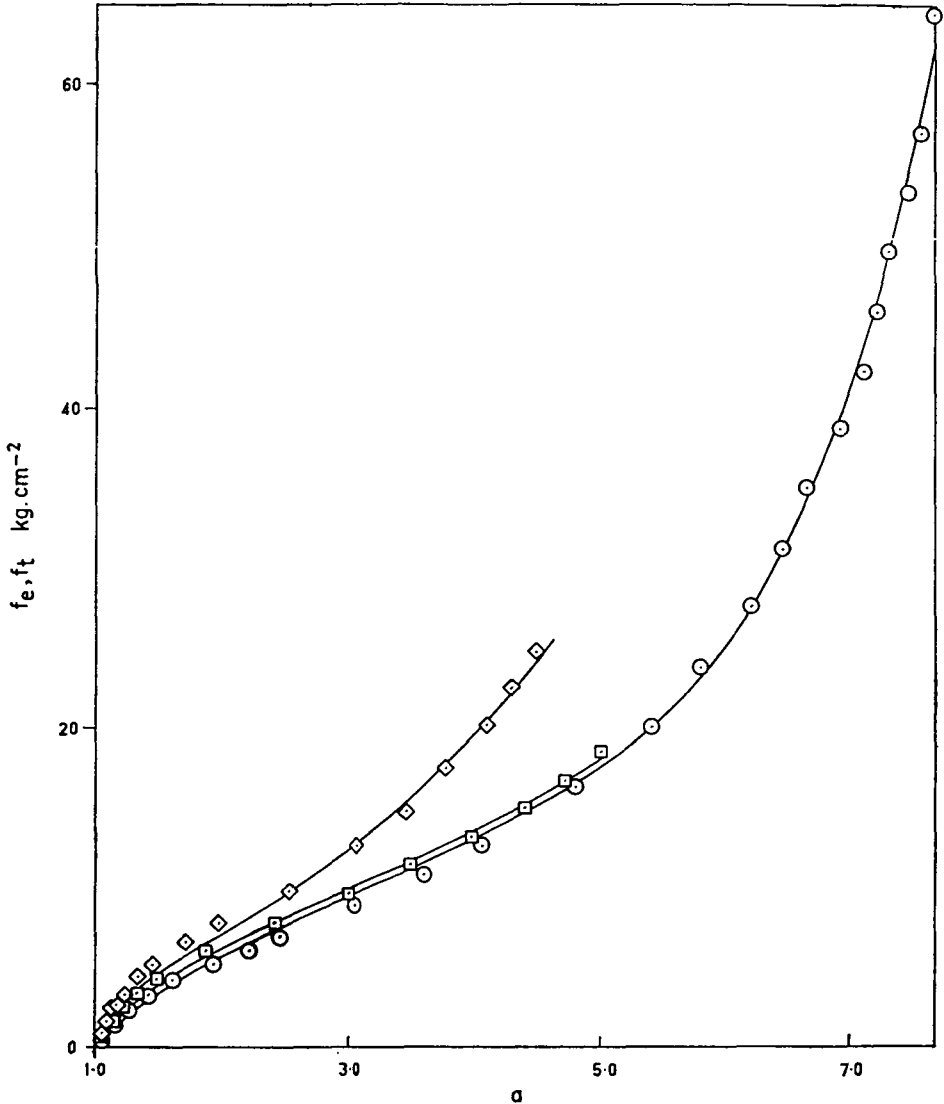


Fig. 4. Comparison with experiment of the response of the modified Mooney material specified by equations (5.5). The values of $\sum |f_e - f_t|$ for experiments 1, 2, 3 are 14.71 (24 points), 3.89 (13 points), 8.63 (16 points).

It should be mentioned that setting $\alpha_1 = 2$ at the outset precludes a close representation of the experimental data for all three experiments at stretches up to about $a = 2$. On comparing Figs. 2 and 3 we see that for experiments 1 and 2 the theoretical representations of the experimental data computed from Ogden's constants (4.5) and the recalculated values (5.4) are of comparable accuracy,

Ogden's results being superior at small strains, but inferior at large strains. In the case of experiment 3, Ogden's correlation of theory and experiment is palpably the closer of the two. It appears, therefore, that the experimental data are best described, on the basis of the strain-energy function (1.1), by taking the smallest positive exponent to be less than 2, a conclusion supported by an analysis of a fresh series of experiments by Jones and Treloar [8, §3]. On the other hand, the closeness of fit produced by the constants (5.4) is not unsatisfactory, and the concept of non-neo-Hookean behaviour at small strains is not, as yet, firmly founded on the kinetic theory of rubber elasticity. Reference to Fig. 4 shows that the account of Treloar's experimental results provided by the second set of recalculated material constants (5.5) is mostly inferior to that given by (5.4). However, it is worthy of note that a fit which is qualitatively correct over the entire range of strains and quantitatively accurate at large strains can be achieved when only one exponent (α_3) is disposable. It is also significant that the addition to the Mooney strain-energy function of a third term which is negligible at small strains nevertheless provides, for all three experiments, the upturn of the force-extension curve at large strains which the Mooney function fails to predict.

We now return to the remaining problems formulated in Section 3.

6. The shrink-fitted tube

(a) Existence and uniqueness of solutions

The axial stretch λ experienced by the shrink-fitted tube is determined, through the constant γ , by equation (3.3), with (3.4) and (3.5). We now prove that the constitutive inequalities (1.2) together with the additional requirements (1.6) guarantee the existence of a unique stable solution for all values of the speed of rotation ω for which the contact stress $\sigma_{rr}(a)$ is compressive.

First, we examine the formula (3.6) for $\sigma_{rr}(a)$. It is a consequence of the definitions (3.5)₁ and (2.15) that $I_1(\gamma; \alpha)$ has the same sign as α when $\gamma > 1$ and the opposite sign when $0 < \gamma < 1$. In view of the inequalities (1.2) it follows that the first term on the right side of (3.6) is negative when $\gamma > 1$, zero when $\gamma = 1$ and positive when $0 < \gamma < 1$. Since the second term on the right of (3.6) is zero when $\omega = 0$ and positive when $\omega > 0$, we conclude that any solution of equation (3.3) must exceed unity if the contact condition (2.16) is to be satisfied when the tube is stationary† or turning sufficiently slowly.

Next we introduce a bounding value $\hat{\omega}$ of the angular speed, defined by

$$\rho \hat{\omega}^2 A^2 q^2 (N^2 - 1) = 4\mu_n (q^{\alpha_n} - q^{-2\alpha_n}). \quad (6.1)$$

† The fact that the search for solutions can be confined to the interval $\gamma > 1$ was overlooked by Chadwick and Haddon [5] when treating the static case of the present problem. Consequently the additional requirements (A1) in their paper are redundant, as are the first members of the two pairs of expressions given on p. 275.

Equations (3.3) to (3.5), with (2.15), then show that if $0 \leq \omega < \hat{\omega}$,

$$J(1) = -\frac{1}{2}\rho\hat{\omega}^2 A^2(N^2-1)^2 < -\frac{1}{2}\rho\omega^2 A^2(N^2-1)^2. \tag{6.2}$$

The asymptotic results

$$j(\gamma; \alpha) \sim \begin{cases} 2(N^2-1)q^{-2-2\alpha}\gamma^{1+\alpha} & \text{when } \alpha > 0 \\ -\frac{4}{2+\alpha}(N^{2+\alpha}-1)q^{-2+\alpha}\gamma^{1-\alpha} & \text{when } \alpha < 0, \alpha \neq -2 \\ -4(\log N)q^{-4}\gamma^3 & \text{when } \alpha = -2 \end{cases} \tag{6.3}$$

$\text{as } \gamma \rightarrow \infty$

are easily derived from equations (3.4) and (3.5). In conjunction with (3.3) and the inequalities (1.2) they tell us that $J(\gamma) \rightarrow \infty$ as $\gamma \rightarrow \infty$. These facts imply that when $0 \leq \omega < \hat{\omega}$ there is at least one solution of equation (3.3) exceeding unity. A sufficient condition for the solution to be unique is $J'(\gamma) > 0$ for all $\gamma > 1$. A detailed investigation similar to that described in [5, App. 1] shows that for $\gamma > 1$

$$j'(\gamma; \alpha) \begin{cases} > 0 & \text{if } \alpha \geq 2, \\ < 0 & \text{if } \alpha \leq -1, \end{cases} \tag{6.4}$$

and it follows from (3.3) that, subject to the restrictions (1.2) and (1.6), $J'(\gamma) > 0$ for $\gamma > 1$. According to the energy criterion stated in Appendix 2 the unique solution guaranteed by this inequality is locally stable.

When $\omega = \hat{\omega}$ we see from (6.1) that the unique solution of equation (3.3) is $\gamma = 1$. Reference to equations (3.6) and (3.5)₁ reveals that $\sigma_{rr}(a)$ is then positive. When $\omega = 0$ equation (3.3) delivers a unique value of γ greater than unity and, as noted above, $\sigma_{rr}(a)$ is then negative. Since $\sigma_{rr}(a)$ is a continuous function of ω we deduce that there is a value $\bar{\omega}$ in the interval $0 < \omega < \hat{\omega}$ at which $\sigma_{rr}(a) = 0$ and such that $\sigma_{rr}(a) < 0$ for all $0 \leq \omega < \bar{\omega}$: $\bar{\omega}$ is the speed of rotation at which the tube loses contact with the spindle and we refer to it henceforth as the *spin-off speed*.

In the course of the foregoing analysis we have shown that the unique solution of equation (3.3) which exists when $0 \leq \omega < \bar{\omega}$ is greater than unity. This means that $\lambda > q^{-2}$, but since $q > 1$ the question of whether or not the tube is shortened by rotation remains unanswered. Equations (3.4), (3.5) and (2.15)₃ give

$$j(q^2; \alpha) = - \int_{(N^2-1+q^2)/N^2}^{q^2} \left\{ q^2 \frac{v^{-1\alpha} - v^{1\alpha}}{v(v-1)} + (q^2-1) \left(\frac{v^{1\alpha} - v^{-1\alpha}}{v-1} \right)^2 \right\} dv \tag{6.5}$$

$$= \int_{(N^2-1+q^2)/N^2}^{q^2} \{ v^{1\alpha} - 1 + q^2(2 - v^{-1} - v^{1\alpha-1}) \} \frac{1 - v^{-1\alpha}}{(v-1)^2} dv. \tag{6.6}$$

The right side of (6.5) is negative when $\alpha < 0$ and the right side of (6.6) is positive when $0 < \alpha \leq 2$. Thus $J(q^2) > 0$ if

$$\alpha_n \leq 2 \quad \text{for each } n.$$

In view of (6.2) these conditions, conjoined with (1.2) and (1.6), suffice for the unique solution of equation (3.3) to lie between q^{-2} and 1, and hence for the tube to shorten. The extended requirements are satisfied by the neo-Hookean and Mooney materials, but not by the Ogden materials specified in equations (4.5), (5.4) and (5.5). However, the numerical results described below show that in fact tubes made of these materials undergo axial contraction for all angular speeds below the spin-off value.†

(b) Numerical results

Calculations have been performed for each of the Ogden materials defined by equations (4.5), (5.4) and (5.5) and for three sizes of tube, given by $N = 1.4, 1.8$ and 2.2 . For each N numerical results have been obtained for six values of the inflation constant q , namely 1.2 (0.2) 2.2. When the radius a of the spindle and the density ρ of the material composing the tube are prescribed, $\hat{\omega}$ can be evaluated from equation (6.1). The bounding speeds corresponding to the chosen (N, q) pairs are given in Table 1, the adopted values of a and ρ being 20 mm and 906.5 kg m^{-3} respectively.

The main computational task is, given $\omega/\hat{\omega}$, to solve equation (3.3) iteratively for γ and then to determine the contact stress from equation (3.6). This programme has been carried out for values of $\omega/\hat{\omega}$ increasing from zero‡ in steps of 0.05, and inverse interpolation in the resulting tabulation of $\sigma_{rr}(a)$ versus $\omega/\hat{\omega}$ yields the spin-off speed as a fraction of $\hat{\omega}$.

The values of $\bar{\omega}/\hat{\omega}$ and the axial stretch at spin-off corresponding to the three materials and the assumed (N, q) values are set out in Table 1. These results display anticipated trends: for each material and each N the spin-off speed and the amount of shortening ultimately suffered by the tube both increase with the inflation constant q , while at each q these quantities both decrease as the thickness constant N increases. As we might expect from the discussion given in Section 5, there is little variation of response among the three materials. Figure 5 shows the variation with $\omega/\hat{\omega}$ of the scaled contact stress for the two Ogden materials specified by equations (4.5) and (5.4) and for selected values of N and q . In each case the contact stress increases monotonically through negative values as the angular speed increases, and again the results for the different materials are closely similar. The general form of the stress distribution in the cylinder is the same for all speeds of rotation in the range $0 \leq \omega < \bar{\omega}$. The detailed study of the static case $\omega = 0$ made in [5, §2(c)] accordingly obviates the need for further comment here.

† See Table 1 below.

‡ In the case of the stationary tube ($\omega = 0$) our calculations reproduce exactly the analogous results reported in [5, §2(c)].

TABLE 1

Shrink-fitted tube: values of the bounding angular velocity $\hat{\omega}$ (s^{-1}), the scaled spin-off speed $\bar{\omega}/\hat{\omega}$ and the axial stretch λ at spin-off for Ogden materials with constants specified in (a) equations (4.5), (b) equations (5.4), (c) equations (5.5).

q	$N = 1.4$			$N = 1.8$			$N = 2.2$		
	$\hat{\omega}$	$\bar{\omega}/\hat{\omega}$	λ	$\hat{\omega}$	$\bar{\omega}/\hat{\omega}$	λ	$\hat{\omega}$	$\bar{\omega}/\hat{\omega}$	λ
1.2 (a)	2620	0.287	0.928	1715	0.354	0.936	1310	0.386	0.940
(b)	2385	0.290	0.928	1562	0.356	0.936	1193	0.389	0.940
(c)	2293	0.296	0.928	1501	0.363	0.936	1147	0.397	0.940
1.4 (a)	4077	0.311	0.870	2669	0.389	0.884	2039	0.430	0.892
(b)	3773	0.311	0.870	2470	0.389	0.883	1887	0.428	0.891
(c)	3591	0.323	0.869	2351	0.403	0.882	1796	0.444	0.890
1.6 (a)	5502	0.328	0.821	3602	0.416	0.839	2751	0.464	0.851
(b)	5206	0.324	0.821	3408	0.410	0.838	2603	0.456	0.849
(c)	4927	0.340	0.820	3226	0.429	0.837	2464	0.477	0.847
1.8 (a)	6996	0.340	0.780	4580	0.436	0.801	3498	0.490	0.815
(b)	6774	0.332	0.779	4435	0.424	0.799	3387	0.475	0.812
(c)	6397	0.351	0.778	4188	0.446	0.797	3199	0.499	0.809
2.0 (a)	8606	0.347	0.744	5634	0.450	0.768	4303	0.509	0.784
(b)	8509	0.337	0.743	5570	0.433	0.765	4254	0.487	0.779
(c)	8038	0.357	0.741	5262	0.457	0.762	4019	0.514	0.775
2.2 (a)	10362	0.352	0.712	6784	0.459	0.738	5181	0.522	0.756
(b)	10424	0.340	0.711	6824	0.439	0.734	5212	0.496	0.750
(c)	9872	0.360	0.709	6463	0.464	0.730	4936	0.523	0.744

7. The freely rotating tube

In our earlier investigations of the rotating cylinder and the shrink-fitted tube we have obtained conditions on the material constants μ_n and α_n in the Ogden strain–energy function (1.1) which guarantee the existence of a unique solution for all relevant angular speeds. The problem of the freely rotating tube presents greater mathematical difficulties because there are now two coupled equations, (3.7) and (3.8), determining the unknown deformation constants λ and γ .† In subsection (a) we establish sufficient conditions for the existence of at least one solution at all speeds of rotation. The additional restrictions on the exponents α_n which we lay down are, however, more severe than their predecessors (1.6) and (1.7), so much so that they exclude the Mooney as well as the neo-Hookean material. The behaviour of freely rotating tubes composed of these materials is investigated in subsections (c) to (e) and instances of both the non-existence and the non-uniqueness of solutions are encountered.

† The problem of the eversion of a tube, discussed in [5], also has this feature.

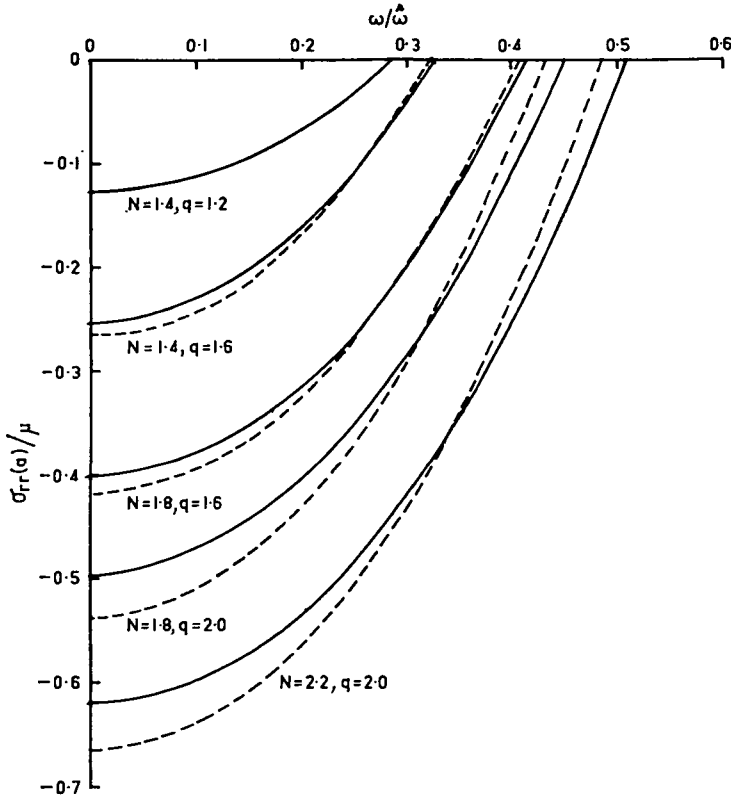


Fig. 5. Shrink-fitted tube: variation of $\sigma_{rr}(a)/\mu$ with $\omega/\hat{\omega}$ for Ogden materials with constants specified in equations (4.5) (solid curves) and equations (5.4) (dashed curves). For $N = 1.4$, $q = 1.2$ the results for the two materials are indistinguishable on the vertical scale shown.

(a) Existence of solutions for a restricted class of Ogden materials

The Ogden materials to be considered here satisfy the constitutive inequalities (1.2) together with the following additional conditions:

$$|\alpha_n| \geq 2 \text{ for each } n; \tag{7.1}$$

$$\alpha_n < 0 \text{ for some } n; \tag{7.2}$$

$$\text{the exponent } \alpha_n \text{ of greatest magnitude exceeds } 2. \tag{7.3}$$

Subject to these requirements we prove that, for all angular speeds, there are positive values of λ and γ satisfying equations (3.7) and (3.8). Certain properties of the auxiliary functions K and L and the integrals I_1 and I_2 which are needed in the proof are listed in parts (a) and (b) of Appendix 1. The derivations of these results from the definitions (3.7), (3.8) and (3.5) are, for the most part, straightforward and details are omitted.

Each of equations (3.7) and (3.8) specifies a family of curves in the (λ, γ) -plane parametrized by ω . We regard equation (3.7) as determining γ as a function of λ , and (3.8) is taken to define λ as a function of γ . The two families of solution curves, which we denote in turn by $\{B_\omega\}$ and $\{C_\omega\}$, thus have the representations $\gamma = \Gamma(\lambda; \omega)$ and $\lambda = \Lambda(\gamma; \omega)$ where

$$K(\lambda, \Gamma(\lambda; \omega)) \equiv \rho\omega^2 A^2(N^2 - 1), \quad L(\Lambda(\gamma; \omega), \gamma) \equiv -\frac{1}{2}\rho\omega^2 A^2(N^2 - 1). \quad (7.4)$$

Since equations (3.7) and (3.8) can only be satisfied by values of λ and γ which make $K(\lambda, \gamma)$ non-negative and $L(\lambda, \gamma)$ non-positive, the statement (A1) allows us to confine attention henceforth to the quarter-plane $Q = \{(\lambda, \gamma): \lambda > 0; \gamma \geq 1\}$.

The results (A1) to (A3) show that, for any fixed positive λ , $K(\lambda, \gamma)$ is a monotone increasing function of γ which is zero at $\gamma = 1$ and unbounded as $\gamma \rightarrow \infty$. For any $\omega \geq 0$ equation (3.7) therefore assigns to the chosen λ exactly one value of γ in the interval $[1, \infty]$: in other words, the function Γ is well defined for all $\lambda > 0$ and $\omega \geq 0$. We deduce from equations (3.7), (A8)₁ and (7.4) that $\Gamma(\lambda, 0) \equiv 1$, and from (7.4)₁ and (A3) that $(\partial\Gamma/\partial\omega)(\lambda; \omega) > 0$.

In geometrical terms we have proved that the curve B_ω meets every line $\lambda = \text{constant}$ in the quadrant Q in a single point, the associated value of γ increasing with ω from unity at $\omega = 0$. The conformation of the family $\{B_\omega\}$ will be established once the behaviour of $\Gamma(\lambda; \omega)$ in the limits $\lambda \downarrow 0$ and $\lambda \rightarrow \infty$ is known, and to this end we invoke the bounds (A9). Let $\hat{\alpha}$ and $\tilde{\alpha}$ be respectively the largest and the smallest of the exponents α_n , and let $\hat{\mu}$ and $\tilde{\mu}$ be the corresponding μ_n 's. The conditions (1.2), (7.1) and (7.3) require that

$$\hat{\alpha} > 2, \quad \tilde{\alpha} \leq -2; \quad \hat{\mu} > 0, \quad \tilde{\mu} < 0, \quad (7.5)$$

and a further consequence of (1.2) is that $\mu_n \lambda^{1-i\alpha_n} I_1(\gamma; \alpha_n) > 0$ for each n . Hence, by appeal to (3.7) and (A9), $K(\lambda, \gamma)$ exceeds both

$$\hat{\mu}(\ln N^2) \lambda^{1-i\hat{\alpha}}(1 - \chi^{-\hat{\alpha}}) \quad \text{and} \quad (-\tilde{\mu})(\ln N^2) \lambda^{1-i\tilde{\alpha}}(1 - \chi^{\tilde{\alpha}}).$$

On equating each of these expressions to the right-hand member of (3.7), using the definition (2.15) and solving for γ , we obtain the equations

$$\gamma = 1 + N^2 \left[\left\{ 1 - \frac{\rho\omega^2 A^2(N^2 - 1)}{\hat{\mu} \ln N^2} \lambda^{-1+i\hat{\alpha}} \right\}^{-1/\hat{\alpha}} - 1 \right] \quad (7.6)$$

and

$$\gamma = 1 + N^2 \left[\left\{ 1 - \frac{\rho\omega^2 A^2(N^2 - 1)}{(-\tilde{\mu}) \ln N^2} \lambda^{-1+i\tilde{\alpha}} \right\}^{1/\tilde{\alpha}} - 1 \right]. \quad (7.7)$$

Let B_ω^1 and B_ω^2 denote the curves in the (λ, γ) -plane given by (7.6) and (7.7) respectively.† By the manner in which they have been introduced, both curves lie

† For a fixed positive ω , B_ω^1 and B_ω^2 are not defined for all $\lambda \geq 0$. However, B_ω^1 is defined for sufficiently small and B_ω^2 for sufficiently large values of λ , and this suffices for the validity of our argument.

above B_ω in Q . This is most easily understood by considering a three-dimensional representation of the functions $K(\lambda, \gamma)$ and $\hat{\mu}(\log N^2) \lambda^{1+\hat{\alpha}}(1 - \chi^{-\hat{\alpha}})$ plotted on the same vertical axis against γ and λ on horizontal axes. Consideration of the intersection of the surfaces so formed with planes parallel to the (λ, γ) -plane makes evident the relative placements of B_ω and B_ω^1 . A similar procedure justifies the stated relationship between B_ω and B_ω^2 . It is plain from (7.6) and (7.5)₁ that B_ω^1 passes through the point $\lambda = 0, \gamma = 1$, and from (7.7) and (7.5) that B_ω^2 approaches the λ -axis ($\gamma = 1$) asymptotically as $\lambda \rightarrow \infty$. These properties also apply to B_ω and the family of solution curves of equation (3.7) accordingly has the form sketched in Fig. 6(a). A closer analysis of equation (3.7) in the limit $\lambda \downarrow 0$ reveals that, for all $\omega > 0$, the gradient $(\partial\Gamma/\partial\lambda)(0; \omega)$ of B_ω at its left extremity is infinite if $2 < \hat{\alpha} < 4$, finite and positive if $\hat{\alpha} = 4$, and zero if $\hat{\alpha} > 4$.

Passing on to the equation (3.8), we first note, with regard to (A4) and (A5), that, for any fixed value of γ not less than unity, $L(\lambda, \gamma)$ is a monotone increasing function of λ , tending to negative infinity as $\lambda \downarrow 0$ and to infinity as $\lambda \rightarrow \infty$. For any $\omega \geq 0$, equation (3.8) therefore assigns to the chosen γ precisely one positive value of λ , rendering the function $\Lambda(\gamma; \omega)$ well defined for all $\gamma \geq 1$ and $\omega \geq 0$. It follows from equation (7.4)₂ and (A5) that $(\partial\Lambda/\partial\omega)(\gamma; \omega) < 0$. Thus the curve C_ω cuts every line $\gamma = \text{constant}$ in the region Q in a single point, the value of λ at the intersection decreasing as ω increases.

It remains to determine the behaviour of C_ω at $\gamma = 1$ and as $\gamma \rightarrow \infty$. Equations (3.8), (A8) and (7.4) give $\Lambda(1; 0) = 1$. Hence $0 < \Lambda(1; \omega) < 1$ for all $\omega > 0$, and on differentiating (7.4)₂ with respect to γ , evaluating at $\gamma = 1$ and making use of (A5) and (A6), we find that $\{(\partial\Lambda/\partial\gamma)(1; \omega)\}^{-1}$, the gradient of C_ω at its lower end, is infinite when $\omega = 0$ and negative when $\omega > 0$. To determine the asymptotic form of C_ω as $\gamma \rightarrow \infty$ we call on the result (A7). Arguing by contradiction we can infer from this equation and (7.4) that, for all $\omega \geq 0$, $\Lambda(\gamma; \omega)$ does not approach zero or a finite limit as $\gamma \rightarrow \infty$. λ and γ must therefore tend to infinity together on C_ω and inspection of (A7) shows that the dominant terms in $L(\lambda, \gamma)$ in this limit are one or more of $T_1 = \hat{\mu}(N^2 - 1) \lambda^{1+\hat{\alpha}} \gamma^{-1}$, $T_2 = -\hat{\mu} \hat{D} \lambda^{1+\hat{\alpha}} \gamma^{-1+\hat{\alpha}}$, $T_3 = (-\tilde{\mu}) \tilde{D} \lambda^{1+\hat{\alpha}} \gamma^{-1+\hat{\alpha}}$, where $\hat{D} = D(\hat{\alpha})$ and $\tilde{D} = D(-\hat{\alpha})$. Since T_1 and T_3 are positive and T_2 is negative, equation (3.8) can hold true only if

- (i) $T_1 + T_2 = 0$ and $T_3/T_2 \rightarrow 0$ as $\lambda, \gamma \rightarrow \infty$, or
- (ii) $T_2 + T_3 = 0$ and $T_1/T_2 \rightarrow 0$ as $\lambda, \gamma \rightarrow \infty$, or
- (iii) $T_1 + T_2 + T_3 = 0$.

Each of these requirements gives rise to a relation of the form

$$\gamma = k\lambda^m, \tag{7.8}$$

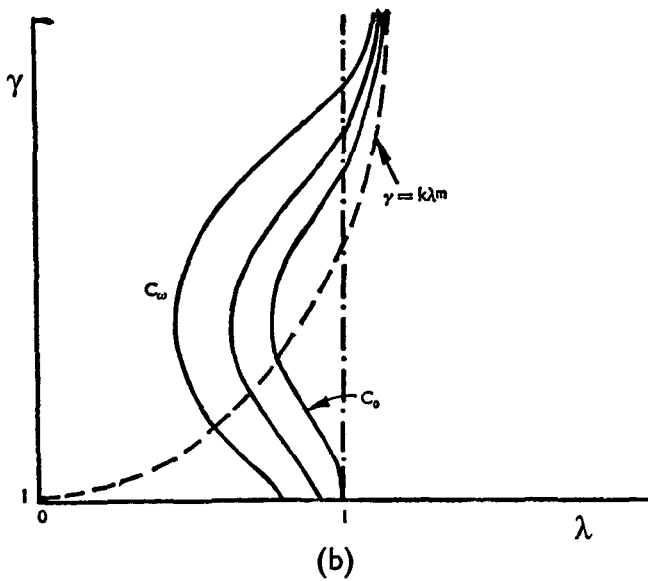
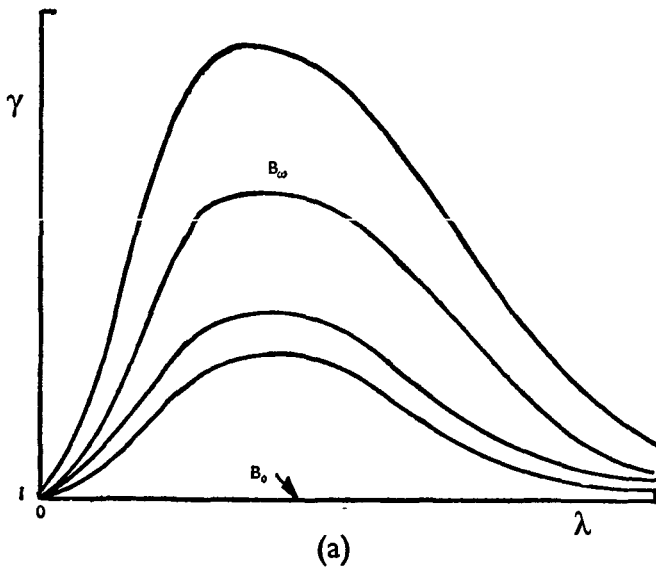


Fig. 6. Freely rotating tube: sketch of the solution curves of (a) equation (3.7) and (b) equation (3.8) for the restricted class of Ogden materials satisfying the conditions (1.2) and (7.1) to (7.3).

describing a curve asymptotic to C_ω . Possibilities (i), (ii) and (iii) apply according as $\hat{\alpha} + 2\tilde{\alpha}$ is positive, negative or zero, and the corresponding values of the constants k and m in (7.8) are given by

$$k = \begin{cases} \{(N^2 - 1)/\hat{D}\}^{2/\hat{\alpha}} & \text{when } \hat{\alpha} + 2\tilde{\alpha} > 0, \\ (-\tilde{\mu}\tilde{D}/\hat{\mu}\hat{D})^{2/(\hat{\alpha} + \tilde{\alpha})} & \text{when } \hat{\alpha} + 2\tilde{\alpha} < 0, \\ [(2\hat{\mu}\hat{D})^{-1}\{(-\tilde{\mu})\tilde{D} + (\tilde{\mu}^2\tilde{D}^2 + 4\hat{\mu}^2\hat{D}(N^2 - 1))^\dagger\}]^{-2/\hat{\alpha}} & \text{when } \hat{\alpha} + 2\tilde{\alpha} = 0, \end{cases}$$

and

$$m = \begin{cases} 3 & \text{when } \hat{\alpha} + 2\tilde{\alpha} \geq 0, \\ (\hat{\alpha} - \tilde{\alpha})/(\hat{\alpha} + \tilde{\alpha}) (> 3) & \text{when } \hat{\alpha} + 2\tilde{\alpha} < 0. \end{cases}$$

We are now able to sketch, in Fig. 6(b), the salient features of the solution curves of equation (3.8), and we observe, on viewing Figs. 6(a) and 6(b) together, that, for all $\omega \geq 0$, the curves B_ω and C_ω intersect in Q .† When $\omega = 0$ the unique point of intersection is $\lambda = 1, \gamma = 1$, representing the undeformed configuration of the tube, and continuity considerations ensure that for small enough speeds of rotation there exists just one solution of equations (3.7) and (3.8). The general question of uniqueness has not been settled, however, and neither have we proved that the tube is invariably shortened by rotation. The fact that $\Gamma(\lambda; \omega)$ and $\Lambda(\gamma; \omega)$ are not monotone functions of their first arguments effectively rules out a frontal attack on these problems.

(b) Numerical results

Of the particular Ogden materials considered in the earlier sections only one, the modified Mooney material specified by equations (5.5), meets the requirements (7.1) to (7.3). Numerical solutions of equations (3.7) and (3.8) have been obtained for this material in respect of a tube with thickness constant $N = 1.4$. Solution curves for the values 2.2, 2.6 and 3.0 of the parameter $\rho\omega^2 A^2$ † are displayed in Fig. 7, where the broken curve marks the C_ω asymptote $\gamma = 1.5736\lambda^3$. Values of λ, γ and q determined by unique intersections of B_ω and C_ω for $\rho\omega^2 A^2 = 1.0$ (0.2) 3.0 are set out in Table 2.

As $\rho\omega^2 A^2$ increases the curves B_ω and C_ω tend to coincidence over an increasing interval of γ as is indicated in Fig. 7. Nevertheless, calculations up to $\rho\omega^2 A^2 = 30$ reveal, for each of the chosen values of this parameter, a unique point of intersection which can be located if a sufficient number of significant figures is retained in the numerical work. This number increases from two when $\rho\omega^2 A^2 = 2$ to five when $\rho\omega^2 A^2 = 30$. However, the material constants in equations (5.5) are given to at

† Alternatively we could conclude the existence proof in formal terms by means of the fixed-point principle used in [5, §3(b)].

‡ These values are in kg cm^{-2} . When $\rho = 906.5 \text{ kg m}^{-3}$ and $A = 20 \text{ mm}$, $\rho\omega^2 A^2 = 1$ corresponds to $\omega = 520.1 \text{ s}^{-1} = 4966 \text{ r.p.m.}$

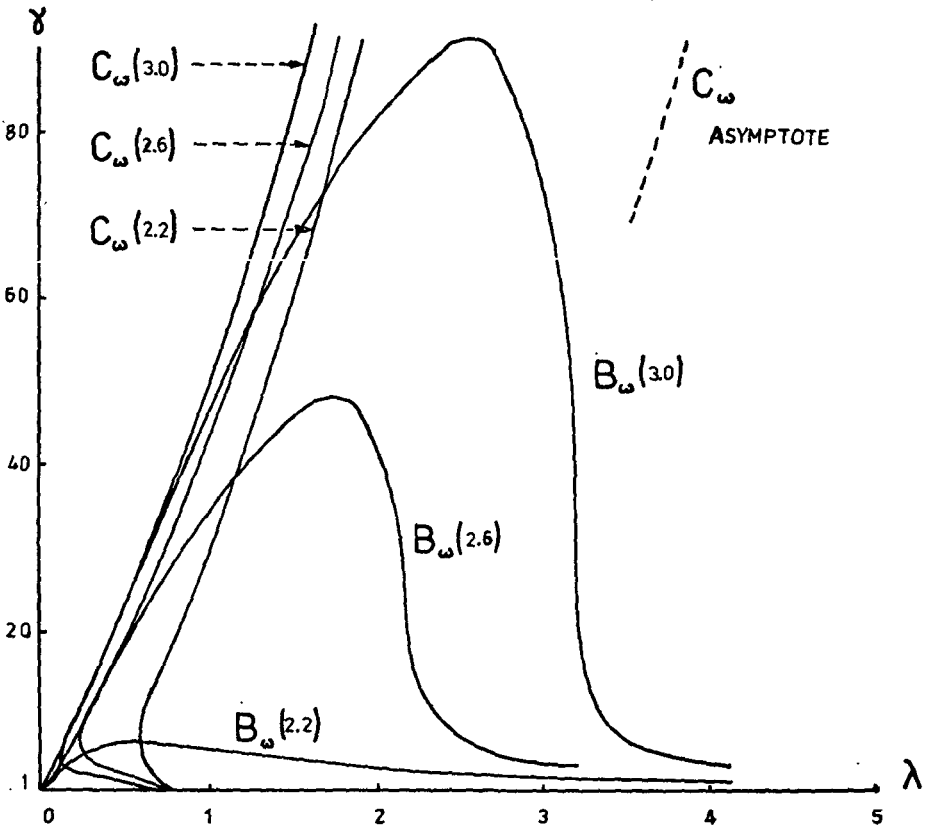


Fig. 7. Freely rotating tube: solution curves of equations (3.7) and (3.8) for the modified Mooney material with constants given by equations (5.5) and thickness constant $N = 1.4$. The parameter in brackets is $\rho\omega^2 A^2$.

TABLE 2

Freely rotating tube: variation of the deformation parameters λ , γ and q with the parameter $\rho\omega^2 A^2$ for the modified Mooney material with constants specified in equations (5.5) and $N = 1.4$.

$\rho\omega^2 A^2$	λ	γ	q
1.0	0.9079	1.451	1.264
1.2	0.8826	1.611	1.351
1.4	0.8531	1.823	1.462
1.6	0.8174	2.122	1.611
1.8	0.7717	2.590	1.832
2.0	0.7063	3.481	2.220
2.2	0.5818	6.408	3.319
2.4	0.4543	13.02	5.353
2.6	0.4199	15.64	6.103
2.8	0.4003	17.15	6.546
3.0	0.3870	18.25	6.867

most three significant figures, so the results for $\rho\omega^2 A^2$ greater than about 2.8 are of questionable validity. The last row of Table 2 shows that by then the tube is in a highly strained state.† With reference to the energy arguments developed in Appendix 2, the Hessian Δ (defined by equation (B10)) is found to decrease through positive values as ω increases. It follows that the material defined by equations (5.5) yields a locally stable solution tending towards neutral stability as the tube is rotated more rapidly.

Since the exponents in equations (1.4), (1.5), (4.5) and (5.4) do not comply with the conditions (7.1) to (7.3) it appears that materials providing more or less acceptable models of rubber-like elasticity may fail to yield a solution, or produce multiple solutions, to the present problem. We now look further into these possibilities by eliciting the nature of the solutions of equations (3.7) and (3.8) for Mooney and neo-Hookean materials.

(c) *Mooney materials*

In the case of a Mooney material, specified by equations (1.5), explicit evaluation of the integrals I_1 and I_2 in equations (3.7) and (3.8) becomes possible. For our present purposes it is convenient to replace (3.8) by the relation

$$\frac{1}{2}K(\lambda, \gamma) + L(\lambda, \gamma) = 0,$$

obtained by eliminating ω . The two equations governing the deformation constants λ and γ can then be expressed by

$$\phi(\gamma) = (1 + \kappa\lambda^2)^{-1}(\omega/\omega_1)^2, \quad \psi(\lambda, \gamma) = 0, \tag{7.9}$$

where

$$\phi(\gamma) \equiv (\ln N^2)^{-1} \left(\frac{1}{\chi} - \frac{1}{\gamma} + \ln \frac{\gamma}{\chi} \right), \tag{7.10}$$

$$\begin{aligned} \psi(\lambda, \gamma) \equiv & 4\lambda^4 + \kappa \left(6 - \frac{1}{\gamma} - \frac{1}{\chi} + \frac{N^2 + 4\gamma - 3}{N^2 - 1} \ln \frac{\gamma}{\chi} \right) \lambda^3 \\ & + \left(-2 - \frac{1}{\gamma} - \frac{1}{\chi} + \frac{N^2 + 1}{N^2 - 1} \ln \frac{\gamma}{\chi} \right) \lambda - 4\kappa, \end{aligned} \tag{7.11}$$

and κ and ω_1 are defined by‡

$$\kappa = -\mu_2/\mu_1, \quad \rho\omega_1^2 A^2(N^2 - 1) = \mu_1 \ln N^2. \tag{7.12}$$

We note that χ is given by equation (2.15) and that $\kappa > 0$ by virtue of the inequalities (4.3). Properties of the functions ϕ and ψ to which appeal is made in the subsequent analysis are assembled in part (c) of Appendix 1.

† For the hollow tube the maximum value of the circumferential principal stretch a_θ occurs at the inner surface $r = a$ and is equal to q .

‡ When $\rho = 906.5 \text{ kg m}^{-3}$, $\mu_1 = 3.625 \times 10^6 \text{ N m}^{-2}$, $A = 20 \text{ mm}$ and $N = 1.4$, we have $\omega_1 = 837.1 \text{ s}^{-1} = 7994 \text{ r.p.m.}$

Equation (7.9) defines a family of curves $\{B_\omega\}$ in the (λ, γ) -plane and (7.9) represents a single curve C . Modifying slightly the notation used in subsection (a), we take B_ω to be given by $\gamma = \Gamma(\lambda; \omega)$ and C by $\lambda = \Lambda(\gamma)$. Then

$$\phi(\Gamma(\lambda; \omega)) \equiv (1 + \kappa\lambda^2)^{-1}(\omega/\omega_1)^2, \quad \psi(\Lambda(\gamma), \gamma) \equiv 0. \quad (7.13)$$

We are justified by the statement (A10) in restricting the search for the intersection of B_ω with C to the quadrant Q of the (λ, γ) -plane.

We start by drawing from equations (7.9) and (7.10) the main features of the curves $\{B_\omega\}$. The results (A10) to (A12) show that $\phi(\gamma)$ is a monotone function, increasing from zero at $\gamma = 1$ towards unity as $\gamma \rightarrow \infty$. It follows from equation (7.13)₁ that $(\partial\Gamma/\partial\lambda)(\lambda; \omega) \leq 0$ and $(\partial\Gamma/\partial\omega)(\lambda; \omega) \geq 0$, the zero values holding together at $\omega = 0$. Since the left side of (7.9)₁ lies between 0 and 1, the ranges of values of λ and ω for which $\Gamma(\lambda; \omega)$ is well defined are restricted. We consider in turn the cases $0 \leq \omega < \omega_1$, $\omega = \omega_1$ and $\omega > \omega_1$.

When $0 \leq \omega < \omega_1$ the right side of equation (7.9) is less than unity for all $\lambda \geq 0$, wherefore $\Gamma(\lambda, \gamma)$ is well defined throughout this interval. For the stationary tube, $\Gamma(\lambda; 0) \equiv 1$, and for $0 < \omega < \omega_1$, $\Gamma(\lambda; \omega)$ decreases monotonically from a finite value at $\lambda = 0$ towards zero as $\lambda \rightarrow \infty$. Curve (i) in Fig. 8 portrays a typical member of $\{B_\omega\}$ in this case. As ω increases from zero, $\Gamma(0; \omega)$ increases from unity and tends to infinity as $\omega \rightarrow \omega_1$, the right side of (7.9) being equal to unity when $\lambda = 1$ and $\omega = \omega_1$. The solution curve B_ω in the case $\omega = \omega_1$ therefore resembles a branch of a rectangular hyperbola and appears in Fig. 8 as curve (ii). When $\omega > \omega_1$ the right side of (7.9)₁ is less than, equal to, or greater than unity according as $\lambda \cong \lambda_1$ where

$$\lambda_1 = \left\{ \kappa^{-1} \left(\frac{\omega^2}{\omega_1^2} - 1 \right) \right\}^{\frac{1}{2}}. \quad (7.14)$$

In this case $\Gamma(\lambda; \omega)$ is well defined in the reduced interval (λ_1, ∞) , approaching infinity as $\lambda \downarrow \lambda_1$ and zero as $\lambda \rightarrow \infty$. Again the solution curves are quasi-hyperbolic and two representatives of $\{B_\omega\}$ are labelled (iii) in Fig. 8.

The properties (A13) to (A15) of $\psi(\lambda, \gamma)$ tell us that, for all $\gamma \geq 1$, the quartic equation (7.9)₂ has exactly one positive real root, situated between 0 and 1. Thus not only is $\Lambda(\gamma)$ well defined for all $\gamma \geq 1$, but C lies entirely in the half-strip $\{(\lambda, \gamma): 0 < \lambda \leq 1, \gamma \geq 1\}$, implying that a freely spinning tube composed of a Mooney material is necessarily shortened by rotation. Equations (7.13) and (7.11) give $\Lambda(1) = 1$, and from (7.13) and (A16) we deduce that $\Lambda'(\gamma) < 0$ for all $\gamma \geq 1$. The asymptotic form of Λ as $\gamma \rightarrow \infty$ is found from equations (7.13) and (7.11) to be

$$\Lambda(\gamma) \sim \{(N^2 - 1)/\ln N^2\}^{\frac{1}{2}} \gamma^{-\frac{1}{2}}.$$

The features of the curve C revealed by these findings are illustrated in Fig. 8.

It is now apparent with reference to Fig. 8, that B_ω intersects C whenever $0 \leq \omega < \omega_1$. As in subsection (a) the governing equations have the unique solution

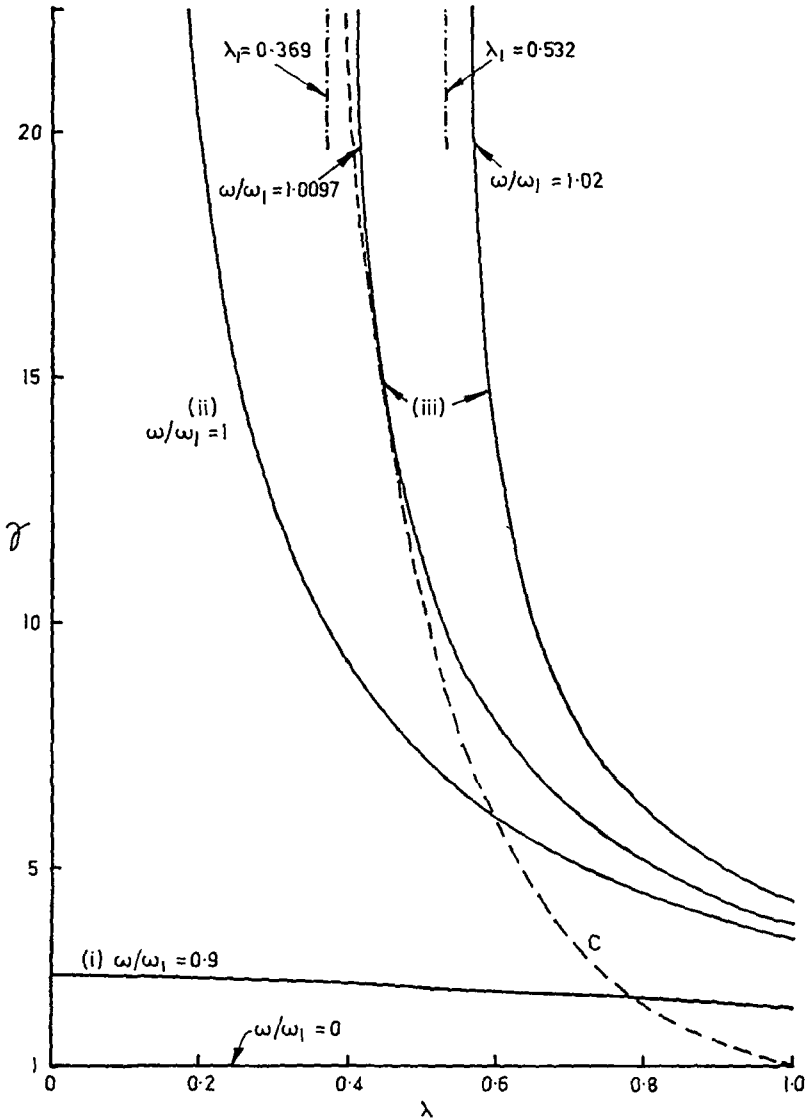


Fig. 8. Freely rotating tube: solution curves of equations (7.9) for a Mooney material with $-\mu_2/\mu_1 = \frac{1}{2}$. The vertical broken lines indicate asymptotes of the curves (iii).

$\lambda = 1, \gamma = 1$ when $\omega = 0$ and the uniqueness property can be extended to a finite range of values of ω on grounds of continuity. B_ω and C do not meet if $\lambda_1 \geq 1$ and no physically meaningful solution of equations (7.9) then exists. The associated range of angular speeds is given by

$$\omega \geq \omega'_1 \quad \text{where} \quad \omega'_1 = (1 + \kappa)^{\frac{1}{2}} \omega_1 = \left\{ \frac{(\mu_1 - \mu_2) \ln N^2}{\rho A^2 (N^2 - 1)} \right\}^{\frac{1}{2}} \quad (7.15)$$

The intermediate range $\omega_1 \leq \omega < \omega'_1$ marks the transition from a situation in which there is at least one solution to one in which no solution exists. Since our analysis is inconclusive in this régime we seek further insight in a numerical study of a particular case.

(d) *Numerical results and discussion*

Equations (7.9) have been solved numerically for a tube with thickness constant $N = 1.4$ composed of a Mooney material for which $\kappa = \frac{1}{7}$. The curve C and the solution curves of equation (7.9)₁ for which $\omega/\omega_1 = 0.9, 1, 1.0097$ and 1.02 are shown in Fig. 8.

There is evidently a unique solution for all angular speeds up to ω_1 and values of the deformation constants at speeds within this range are given in Table 3. As ω

TABLE 3
Freely rotating tube: variation of the deformation parameters λ, γ and q with the scaled angular speed for a Mooney material with $-\mu_2/\mu_1 = \frac{1}{7}$ and $N = 1.4$.

ω/ω_1	λ	γ	q
0.1	0.9985	1.006	1.004
0.2	0.9939	1.025	1.015
0.3	0.9859	1.058	1.036
0.4	0.9741	1.109	1.067
0.5	0.9579	1.184	1.112
0.6	0.9358	1.295	1.176
0.7	0.9056	1.466	1.272
0.8	0.8623	1.757	1.428
0.9	0.7923	2.376	1.732
1.0	0.5956	6.101	3.201

increases from zero the deformation of the tube, consisting of radial inflation accompanied by axial contraction, is at first gradual, but progressive “softening” occurs, as in the steady rotation of a cylinder made of the Ogden material specified in equations (4.5) (Section 4(b)). This tendency reaches an advanced stage at speeds in excess of about $0.7\omega_1$, and as the critical value ω_1 is approached the tube offers no appreciable resistance to further deformation. At $\omega = \omega_1$ the deformation is severe, the internal radius being increased more than three-fold and the length reduced to 60% of its initial value.

The member of $\{B_\omega\}$ for which $\omega = \omega_1$ intersects C at the point $\lambda = 0.5956, \gamma = 6.101$, and both curves are asymptotic to the γ -axis as $\gamma \rightarrow \infty$. Thus there are two solutions when $\omega = \omega_1$, one corresponding to a deformed configuration in which the radii of the tube tend to infinity and the length to zero. As ω increases further this bifurcation phenomenon persists, the two points at which B_ω cuts C approaching one another until, when $\omega = \omega_2$, they coalesce and B_ω touches C . In

the present case, $\omega_2/\omega_1 = 1.0097$ and the point of contact is given by $\lambda = 0.4518$, $\gamma = 14.42$ (with $q = 5.649$). When $\omega > \omega_2$ the curves B_ω and C are disjoint and no solution exists.† As shown in Appendix 2 the energy criterion implies that the solution is locally stable when $0 \leq \omega < \omega_1$. In the range $\omega_1 \leq \omega < \omega_2$ for which bifurcation occurs the solution with the larger value of λ is locally stable while the other solution is neutrally stable. With the values for ρ , μ_1 and A given in the footnote relating to equation (7.12), $\omega_2 = 8072$ r.p.m. The corresponding value of $\rho\omega_2^2 A^2$ is $2.6408 \text{ kg cm}^{-2}$ which invites comparison with the value 2.8 kg cm^{-2} of $\rho\omega^2 A^2$ noted in subsection (b) in connection with the approach to neutral stability of a freely spinning tube composed of the modified Mooney material defined by equations (5.5).

The critical speed of rotation ω_1 thus marks the onset of a curious type of bifurcation which terminates, after an additional rise of less than 1% in the angular speed, in the entire disappearance of the solution. This behaviour, which seems to have no parallel in previous studies of Mooney materials at finite strain, shows that the propensity of the Mooney strain–energy function towards physically realistic response may not be without limitations. It is possible, however, as in the case of the solid cylinder, that bifurcation into an asymmetric state of deformation may occur before the critical angular velocity is reached. Following this line of conjecture we observe from (7.12)₂ that ω_1 decreases as N increases at fixed internal radius A , indicating that the critical speed is a decreasing function of the thickness. Since thick tubes are generally more stable than thinner ones this suggests that the interpretation of ω_1 as marking the onset of instability must be viewed with some caution.

(e) *Neo-Hookean materials*

In conclusion we note the effect on the solution obtained in subsection (c) of setting $\mu_1 = \mu$, $\mu_2 = 0$ (and hence $\kappa = 0$). Equations (7.9) now assume the decoupled form

$$\phi(\gamma) = (\omega/\omega_1)^2, \quad \lambda^3 = \frac{1}{4} \left(2 + \frac{1}{\gamma} + \frac{1}{\chi} - \frac{N^2 + 1}{N^2 - 1} \ln \frac{\gamma}{\chi} \right), \tag{7.16}$$

γ and λ being determined successively by (7.16)₁ and (7.16)₂. The first equation has a unique solution if and only if $0 \leq \omega < \omega_1$, γ increasing monotonically from unity at $\omega = 0$ towards infinity as $\omega \rightarrow \omega_1$. Equation (7.16) gives $d\lambda/d\gamma < 0$, whence λ decreases monotonically from unity as ω increases from zero. It follows that

$$\lambda^3 \rightarrow \frac{1}{2} - \frac{(N^2 + 1) \ln N^2}{4(N^2 - 1)} = -\frac{1}{4(N^2 - 1)} \int_0^{N^2 - 1} \left\{ -\ln \left(1 - \frac{x}{1+x} \right) - \frac{x}{1+x} \right\} dx < 0$$

† Equation (7.15) supplies the upper bound $\omega'_1 = 1.0690\omega_1$ for ω_2 .

as $\omega \rightarrow \omega_1$, demonstrating that λ becomes zero when ω reaches a critical value $\omega_3 < \omega_1$. For a tube with thickness constant $N = 1.4$, $\omega_3/\omega_1 = 0.9998$.

In summary, equations (7.16) have exactly one solution for all angular speeds up to ω_3 and no meaningful solution when $\omega \geq \omega_3$. As indicated in Appendix 2 the unique solution for $\omega < \omega_3$ is stable. The bifurcation effect encountered in subsection (d) is absent in the neo-Hookean case.

Acknowledgements

Our thanks are due to Mr. E. W. Haddon for assistance with the numerical work described in Section 5 and to the Science Research Council of the United Kingdom for the award of a Studentship to the second-named author. We are also obliged to a referee for some helpful comments.

Appendix 1

Properties of auxiliary functions

(a) *The functions K and L*

For all $\lambda > 0$,

$$K(\lambda, \gamma) \cong 0 \quad \text{according as } \gamma \cong 1, \tag{A1}$$

$$K(\lambda, \gamma) \rightarrow \infty \quad \text{as } \gamma \rightarrow \infty, \tag{A2}$$

$$\frac{\partial K}{\partial \gamma}(\lambda, \gamma) > 0 \quad \text{for all } \gamma \geq 1. \tag{A3}$$

The restrictions on the material constants μ_n and α_n used in proving these results are, in turn, (1.2); (1.2) and (7.3); and (1.2) and (7.1).

For all $\gamma \geq 1$,

$$L(\lambda, \gamma) \rightarrow -\infty \quad \text{as } \lambda \downarrow 0, \quad L(\lambda, \gamma) \rightarrow \infty \quad \text{as } \lambda \rightarrow \infty, \tag{A4}$$

$$\frac{\partial L}{\partial \lambda}(\lambda, \gamma) > 0 \quad \text{for all } \lambda > 0, \tag{A5}$$

$$\frac{\partial L}{\partial \gamma}(\lambda, 1) \begin{cases} > 0 & \text{when } 0 < \lambda < 1, \\ = 0 & \text{when } \lambda = 1. \end{cases} \tag{A6}$$

For each of (A4) to (A6) the basic inequalities (1.2) are needed and the additional requirements (7.1) to (7.3) are also used in proving (A4) and (A5).

For all $\lambda > 0$,

$$L(\lambda, \gamma) = \mu_n[(N^2 - 1)\lambda^{1+\alpha_n}\gamma^{-1}\{1 + O(\gamma^{-1})\} - \lambda^{1-\frac{1}{2}\alpha_n}\gamma^{-1+\frac{1}{2}\alpha_n}\{D(\alpha_n) + O(\gamma^{-1})\} - \lambda^{1-\frac{1}{2}\alpha_n}\gamma^{-1-\frac{1}{2}\alpha_n}\{D(-\alpha_n) + O(\gamma^{-1})\}] \tag{A7}$$

as $\gamma \rightarrow \infty$, where

$$D(\alpha) = \begin{cases} \frac{N^{2-\alpha} - 1}{2 - \alpha} & \text{when } \alpha \neq 2, \\ \ln N^2 & \text{when } \alpha = 2. \end{cases}$$

(b) *The integrals I_1 and I_2*

$$\left. \begin{aligned} I_1(\gamma; \alpha) &= \alpha(1 - N^{-2})(\gamma - 1) + O((\gamma - 1)^2) \\ I_2(\gamma; \alpha) &= \frac{1}{4}\alpha^2(1 - N^{-2})(\gamma - 1) + O((\gamma - 1)^2) \end{aligned} \right\} \text{ as } \gamma \downarrow 1, \tag{A8}$$

$$\operatorname{sgn} \alpha I_1(\gamma; \alpha) > (\ln N^2)(1 - \chi^{-|\alpha|}) \quad \text{if } |\alpha| \geq 2. \tag{A9}$$

(c) *The functions ϕ and ψ*

$$\phi(\gamma) \cong 0 \quad \text{according as } \gamma \cong 1, \tag{A10}$$

$$\phi(\gamma) \rightarrow 1 \quad \text{as } \gamma \rightarrow \infty, \tag{A11}$$

$$\phi'(\gamma) > 0 \quad \text{for all } \gamma > 0. \tag{A12}$$

For all $\gamma \geq 1$,

$$\psi(0, \gamma) < 0, \tag{A13}$$

$$\psi(1, \gamma) > 0. \tag{A14}$$

For all $\lambda > 0$ and $\gamma \geq 1$,

$$\frac{\partial^2 \psi}{\partial \lambda^2}(\lambda, \gamma) > 0, \tag{A15}$$

$$\frac{\partial \psi}{\partial \lambda}(\lambda, \gamma) - \frac{1}{\lambda} \psi(\lambda, \gamma) > 0, \quad \frac{\partial \psi}{\partial \gamma}(\lambda, \gamma) > 0. \tag{A16}$$

Appendix 2

Energy considerations

In this appendix we calculate the total potential energy V of the rotating tube or cylinder and examine the extrema of V . The conditions for an extremum reproduce the equations for the deformation constants derived in Section 3 while the possible types of extrema determine the status of the deformation in regard to local stability. Attention is again confined to shape-preserving deformations, depending only on the radial coordinate r .

The deformation of a body rotating with constant angular velocity ω about a fixed axis is the same as that of the identical stationary body acted on by a body force $r\omega^2$ per unit mass directed radially outwards from the axis. The total potential

energy of the body is hence the total strain energy less the work done by the body force in passing from the undeformed to the deformed state. For a tube,

$$V = 2\pi L \int_A^B WR dR - \pi\rho\omega^2 \left(l \int_a^b r^3 dr - L \int_A^B R^3 dR \right), \tag{B1}$$

with the notation introduced in Section 2(a).

Substituting into (B1) the expression (3.1) for the Ogden strain–energy function and recalling the definitions (2.3), (2.15) and (3.2) we find that

$$\begin{aligned} (N^2/\pi LB^2) V &= (\mu_n/\alpha_n) \{ (N^2 - 1)(\lambda^{\alpha_n} + 2\lambda^{-\frac{1}{2}\alpha_n} - 3) + (\gamma - 1)\lambda^{-\frac{1}{2}\alpha_n} I_2(\gamma; \alpha_n) \} \\ &\quad - \frac{1}{4}\rho\omega^2 B^2 (1 - N^{-2}) \{ \lambda^{-1}(N^2 - 1) + 2q^2 - N^2 - 1 \}, \end{aligned} \tag{B2}$$

I_2 being given by equation (3.5)₂. For the cylinder and the shrink-fitted tube V is a function of λ only. In the case of the unconstrained tube, however, V is a function of λ and γ , and q^2 must then be replaced by γ/λ .

(a) *The solid cylinder*

Letting a and A tend to zero in (B2) we obtain

$$(1/\pi LB^2) V(\lambda) = (\mu_n/\alpha_n) (\lambda^{\alpha_n} + 2\lambda^{-\frac{1}{2}\alpha_n} - 3) - \frac{1}{4}\rho\omega^2 B^2 (\lambda^{-1} - 1), \tag{B3}$$

whence

$$(1/\pi LB^2) \lambda^2 V'(\lambda) = M(\lambda) + \frac{1}{4}\rho\omega^2 B^2, \quad (1/\pi LB^2) (\lambda^2 V'(\lambda))' = M'(\lambda), \tag{B4}$$

the function M being defined in (3.9). Evidently a root of equation (3.9) is an extremum of $V(\lambda)$ and a root represented by a point on the graph of $-\mu^{-1}M(\lambda)$ (see Fig. 1) at which the gradient is negative (resp. positive) corresponds to a configuration which is locally stable (resp. unstable). A maximum or minimum point of $M(\lambda)$ is associated with neutral stability. An inspection of the curves in Fig. 1 now leads directly to the conclusions stated in Section 4(c).

(b) *The shrink-fitted tube*

In this case equation (B2) yields

$$\left. \begin{aligned} (2N^2/\pi LB^2) \lambda^2 V'(\lambda) &= J(\gamma) + \frac{1}{2}\rho\omega^2 A^2 (N^2 - 1)^2, \\ (2N^2/\pi LB^2) (\lambda^2 V'(\lambda))' &= q^2 J'(\gamma), \end{aligned} \right\} \tag{B5}$$

use being made of equations (3.3) to (3.5). We see from (B5) that a root of equation (3.3) is a minimum value of $V(\lambda)$ if $J'(\gamma)$, evaluated at the root, is positive. The deformation associated with the root is then locally stable and the assertion made in Section 6(a) is justified.

(c) *The freely rotating tube*

The potential energy is now a function of λ and γ and the standard criteria for maxima, minima and saddle points apply. Let

$$\bar{V}(\lambda, \gamma) = (2/\pi LA^2) V(\lambda, \gamma). \tag{B6}$$

Then it follows from (B2) with the use of equations (3.7) and (3.8) that

$$\left. \begin{aligned} \lambda^2(N^2 - 1 + 2\gamma)^{-1} \bar{V}_\lambda(\lambda, \gamma) &= L(\lambda, \gamma) + \frac{1}{2} \rho \omega^2 A^2(N^2 - 1), \\ \lambda \bar{V}_\gamma(\lambda, \gamma) &= K(\lambda, \gamma) - \rho \omega^2 A^2(N^2 - 1), \end{aligned} \right\} \quad (\text{B7})$$

a suffix notation being employed for partial derivatives. These results confirm that a root of equations (3.7) and (3.8) is an extremum of the potential energy. The values of the second derivatives of \bar{V} at such a root are given by

$$\left. \begin{aligned} \lambda^2(N^2 - 1 + 2\gamma)^{-1} \bar{V}_{\lambda\lambda} &= L_\lambda, & \lambda \bar{V}_{\lambda\gamma} &= K_\lambda, \\ \lambda^2(N^2 - 1 + 2\gamma)^{-1} \bar{V}_{\gamma\lambda} &= L_\gamma, & \lambda \bar{V}_{\gamma\gamma} &= K_\gamma. \end{aligned} \right\} \quad (\text{B8})$$

Denoting by m_B and m_C the gradients $d\gamma/d\lambda$ of the solution curves B_ω and C_ω of equations (3.7) and (3.8) respectively, we readily obtain, with the aid of (B8), the relations

$$m_B = -K_\lambda/K_\gamma = -\bar{V}_{\lambda\gamma}/\bar{V}_{\gamma\gamma}, \quad m_C = -L_\lambda/L_\gamma = -\bar{V}_{\lambda\lambda}/\bar{V}_{\gamma\lambda}. \quad (\text{B9})$$

Hence

$$\Delta = \bar{V}_{\lambda\lambda} \bar{V}_{\gamma\gamma} - (\bar{V}_{\lambda\gamma})^2 = \{(m_C/m_B) - 1\} \bar{V}_{\lambda\gamma}^2, \quad (\text{B10})$$

proving that Δ has the same sign as $(m_C/m_B) - 1$.

For the modified Mooney material specified by equations (5.5) it appears from the numerical results illustrated in Fig. 7 that $m_C/m_B > 1$ at a solution of equations (3.7) and (3.8). Thus $\Delta > 0$ and the inequalities (A5) and (A3) imply, via (B8), that $\bar{V}_{\lambda\lambda} > 0$, $\bar{V}_{\gamma\gamma} > 0$. The solution evidently minimizes the potential energy and is locally stable. The tendency towards neutral stability, mentioned in Section 7(b), arises from the steady diminution of m_C/m_B towards unity as ω increases.

In the case of a Mooney material the calculations described above lead to the explicit formulae

$$\left. \begin{aligned} m_B &= -\frac{2\kappa\lambda}{1 + \kappa\lambda^2} \left(\frac{\chi^{-2} - \gamma^{-2}}{\gamma - 1} \right)^{-1} \left(\frac{1}{\chi} - \frac{1}{\gamma} + \ln \frac{\gamma}{\chi} \right), \\ m_C &= -\frac{1}{2\kappa} \left(\frac{1}{\chi} - \frac{1}{\gamma} + \ln \frac{\gamma}{\chi} \right)^{-1} \left[6(N^2 - 1) + 2\kappa\lambda^{-2} \{ (N^2 - 1)(\lambda^{-2} + 2\lambda) \right. \\ &\quad \left. + \lambda(\gamma - 1) \ln \frac{\gamma}{\chi} \right], \end{aligned} \right\} \quad (\text{B11})$$

where (λ, γ) is a solution of equations (7.9). The numerical results presented in Fig. 8 show that when there is just one solution (that is, for $0 \leq \omega < \omega_1$), $m_C/m_B > 1$. Since $\bar{V}_{\lambda\lambda}$ and $\bar{V}_{\gamma\gamma}$ are positive for all ω this solution is locally stable. When two solutions exist (that is, for $\omega_1 \leq \omega < \omega_2$), the one for which λ is largest is similarly stable. For the other solution $m_C/m_B < 1$ and a state of neutral stability is indicated.

When the strain energy is neo-Hookean

$$\left. \begin{aligned} \bar{V}_{\lambda\lambda} &= 6\mu(N^2 - 1) > 0, & \bar{V}_{\gamma\gamma} &= \mu\lambda^{-1} \left(\frac{X^{-2} - \gamma^{-2}}{\gamma - 1} \right) > 0, \\ \bar{V}_{\lambda\gamma} &= 0. \end{aligned} \right\} \quad (\text{B12})$$

Hence $\Delta > 0$ and when a solution exists it is locally stable.

REFERENCES

- [1] H. Alexander, "Tensile instability of initially spherical balloons", *Int. J. Engng Sci.* 9 (1971), 151–162.
- [2] H. Alexander, "The tensile instability of an inflated cylindrical membrane as affected by an axial load", *Int. J. Mech. Sci.* 13 (1971), 87–95.
- [3] P. Chadwick, "Aspects of the dynamics of a rubberlike material", *Q. Jl Mech. Appl. Math.* 27 (1974), 263–285.
- [4] P. Chadwick and C. F. M. Creasy, "Some existence-uniqueness results for problems of finite elastic bending", *Q. Jl Mech. Appl. Math.* 30 (1977), 187–202.
- [5] P. Chadwick and E. W. Haddon, "Inflation-extension and eversion of a tube of incompressible isotropic elastic material", *J. Inst. Maths Applies* 10 (1972), 258–278.
- [6] A. E. Green and R. T. Shield, "Finite elastic deformation of incompressible isotropic bodies", *Proc. Roy. Soc. A* 202 (1950), 407–419.
- [7] A. E. Green and W. Zerna, *Theoretical Elasticity*, Oxford University Press (1st ed., 1954).
- [8] D. F. Jones and L. R. G. Treloar, "The properties of rubber in pure homogeneous strain", *J. Phys. D: Appl. Phys.* 8 (1975), 1285–1304.
- [9] J. K. Knowles and M. T. Jakub, "Finite dynamic deformations of an incompressible elastic medium containing a spherical cavity", *Arch. Ration. Mech. Analysis* 18 (1965), 367–378.
- [10] R. W. Ogden, "Large deformation isotropic elasticity—on the correlation of theory and experiment for incompressible rubberlike solids", *Proc. Roy. Soc. A* 326 (1972), 565–584.
- [11] R. W. Ogden and P. Chadwick, "On the deformation of solid and tubular cylinders of incompressible isotropic elastic material", *J. Mech. Phys. Solids* 20 (1972), 77–90.
- [12] R. W. Ogden, P. Chadwick and E. W. Haddon, "Combined axial and torsional shear of a tube of incompressible elastic material", *Q. Jl Mech. Appl. Math.* 26 (1973), 23–41.
- [13] J. C. Patterson and J. M. Hill, "The stability of a solid rotating neo-Hookean cylinder", *Mech. Research Comm.* (1977), to appear.
- [14] L. R. G. Treloar, "Stress-strain data for vulcanised rubber under various types of deformation", *Trans. Faraday Soc.* 40 (1944), 59–70.
- [15] L. R. G. Treloar, *The Physics of Rubber Elasticity*, Oxford University Press (3rd ed., 1975).

School of Mathematics and Physics

University of East Anglia

Norwich

England

and

Department of Mathematics

University of Queensland

St Lucia, Q. 4067

Australia